Cancer Science
The official journal of the Japanese Cancer Association JCA

Phase I/II study of decitabine in patients with myelodysplastic syndrome: A multi-center study in Japan

Yasuhiro Oki,[1,15] Yutaka Kondo,[2] Kazuhito Yamamoto,[1] Michinori Ogura,[3] Masanobu Kasai,[3] Yukio Kobayashi,[4] Takashi Watanabe,[4] Naokuni Uike,[5] Kazuma Ohyashiki,[6] Shin-ichiro Okamoto,[7] Kazunori Ohnishi,[8] Akihiro Tomita,[9] Yasushi Miyazaki,[10] Kaoru Tohyama,[11] Harumi Y. Mukai,[12] Tomomitsu Hotta[13] and Masao Tomonaga[14]

[1]Department of Hematology and Cell Therapy, Aichi Cancer Center Hospital, Nagoya; [2]Division of Molecular Oncology, Aichi Cancer Center Research Institute, Nagoya; [3]Department of Hematology and Oncology, Nagoya Daini Red Cross Hospital, Nagoya; [4]Hematology Division, National Cancer Center Hospital, Tokyo; [5]Department of Hematology, National Hospital Organization Kyushu Cancer Center, Fukuoka; [6]Division of Hematology, Tokyo Medical University Hospital, Tokyo; [7]Division of Hematology, Keio University Hospital, Tokyo; [8]Oncology Center, Hamamatsu University School of Medicine, Hamamatsu; [9]Department of Hematology and Oncology, Nagoya University Graduate School of Medicine, Nagoya; [10]Department of Hematology, Nagasaki University Hospital, Nagasaki; [11]Clinical Pathology and Laboratory Medicine, Kawasaki Medical School Hospital, Kurashiki; [12]Janssen Pharmaceutical K.K. Tokyo; [13]National Hospital Organization Nagoya Medical Center, Nagoya; [14]Japanese Red Cross Nagasaki Genbaku Hospital, Nagasaki, Japan

(Received May 17, 2012/Revised July 10, 2012/Accepted July 21, 2012/Accepted manuscript online July 21, 2012/Article first published online September 14, 2012)

The management of myelodysplastic syndrome (MDS) remains challenging. We performed a phase I/II study to evaluate the safety and efficacy of decitabine in patients with MDS in Japan. Patients with MDS with red cell transfusion dependence or 5–30% blasts in marrow and with an International Prognostic Scoring System score of intermediate-1 or higher were eligible. Patients received intravenous decitabine at 15 or 20 mg/m^2 daily for 5 days every 4 weeks. A total of 37 patients were enrolled. Three patients received 15 mg/m^2 and experienced no dose limiting toxicity during the first cycle. Thirty-four patients received 20 mg/m^2. Grade 3 or greater non-hematologic toxicities included cerebral infarction (n = 1), subdural hematoma (n = 1), elevated blood glucose (n = 1), and pulmonary hypertension (n = 1). At 20 mg/m^2, complete response, partial response, and hematologic improvement were observed in 7 (20.6%), 2 (5.9%), and 7 (20.6%) patients, respectively. Complete cytogenetic response was observed in 30% of evaluable 20 patients. The median number of cycles to clinical response was 4 (range 4–8), and duration of remission was 474+ days (range 294–598+). The 2-year rate of acute myeloid leukemia-free survival was 52%. Correlative studies revealed hypomethylation in multiple genes in peripheral blood cells after treatment. Hypomethylation was generally more profound in CD15 + peripheral blood cells, which reflects myeloid cells, than in peripheral blood mononuclear cells. In summary, decitabine was safe and demonstrated efficacy in Japanese patients with high-risk MDS. This trial was registered at ClinicalTrials.gov (NCT00796003). (*Cancer Sci* 2012; 103: 1839–1847)

Myelodysplastic syndrome (MDS) is a heterogeneous group of hematopoietic stem cell disorders presenting as cytopenias and dysplastic hematopoiesis with or without increased blast cells.[1] The disease is associated with a dismal outcome due to progression of cytopenias or transformation to acute leukemia. Management of MDS varies depending on a patient's age, degree of cytopenias, performance status and estimated risk of disease progression[1] as assessed by, for example, the International Prognostic Scoring System (IPSS) score.[2]

Development of MDS is a multistep event. One important mechanism involved is epigenetic change, such as promoter DNA methylation.[3] Frequent methylation often confers a poor prognosis.[4] In recent years, treatment with DNA methyltransferase inhibitors has been studied extensively in the management of MDS. Two drugs in this class, azacitidine[5] and decitabine,[6–8] have been approved in the management of MDS in multiple countries. However, very little data exist regarding treatment of Asian patients with decitabine.[9] Therefore, we conducted a phase I/II study in Japan to assess the safety and efficacy of decitabine in Japanese patients with high-risk MDS. We also performed correlative methylation analysis using 3-fucosyl-*N*-acetyl-lactosamine (CD15)-positive myeloid cells selected from the peripheral blood of patients undergoing treatment with decitabine.

Materials and Methods

This open-label multicenter phase I/II study of decitabine in patients with MDS was approved by the institutional review boards of each participating institution and was conducted in compliance with the International Conference on Harmonisation Good Clinical Practice guidelines (ClinicalTrials.gov identifier: NCT00796003).

Phase I: The primary objective was to assess the safety of intravenous decitabine at 15 and 20 mg/m^2 administered over 1 h daily for 5 days every 4 weeks. Secondary objectives were pharmacokinetic and pharmacodynamic assessments during the first cycle of treatment.

Phase II: The primary objective was to evaluate patient response (rates of complete response [CR] and partial response [PR]). Secondary objectives were time to response, response duration, time to acute myelogenous leukemia (AML) or death, transfusion dependency, and cytogenetic response.

Patients. Eligibility criteria included the following: diagnosis of MDS based on French-American-British (FAB) morphologic classification, including refractory anemia (RA), RA with ringed sideroblasts (RARS), RA with excess blasts (RAEB), RAEB in transformation and chronic myelomonocytic leukemia (CMML); patients with RA or RARS were to have required red blood cell transfusion more than once every 4 weeks, while patients with CMML were to have a white blood cell count of <13 000/mm^3; IPSS assessment of intermediate or high risk; age 20 years or older; Eastern Cooperative Oncology Group (ECOG) performance status of 0–2; and normal organ functions including creatinine $\leq$ 176.8 μM (2 mg/dL), bilirubin $\leq$ 25.7 μM (1.5 mg/dL) and aspartate

[15]To whom correspondence should be addressed.
E-mail: yoki@mdanderson.org

doi: 10.1111/j.1349-7006.2012.02386.x

aminotransferase and alanine aminotransferase levels $\leq 2 \times$ the upper limit of normal.

Patients were ineligible if they had: bone marrow blast percentage $\geq 30\%$ on local marrow review; prior chemotherapy with cytarabine ≥ 1 g/m^2; or other serious comorbidities, active infectious disease, autoimmune cytopenia, hepatitis B surface antigen positivity, hepatitis C antibody positivity or HIV antibody positivity. Pregnant or lactating female patients were also ineligible.

Treatment. Two decitabine doses and schedules have been recommended in previous studies in MDS, namely 15 mg/m^2 over 3 h every 8 h for 3 days every 6-week cycle[6] and 20 mg/m^2 over 1 h daily for 5 days every 4-week cycle.[7,8] Because the latter method has shown clinical efficacy and convenience in the outpatient setting, we chose the 5-day dosing schedule for this study. We started treatment at 15 mg/m^2 daily, escalating to 20 mg/m^2 after safety was assessed.

Treatment was repeated every 4 weeks in the absence of dose limiting toxicity (DLT, defined below) or disease progression. In order to receive the next cycle of treatment, a patient was required to have normal organ function as defined above. If the patient did not meet these criteria on day 29, a maximum 2-week delay was allowed. Treatment was also delayed if the patient had febrile neutropenia, grade 3 or 4 infection with neutropenia, or $\geq$ grade 2 bleeding. If, by day 43, the patient did not meet the above criteria, the patient was taken off the study.

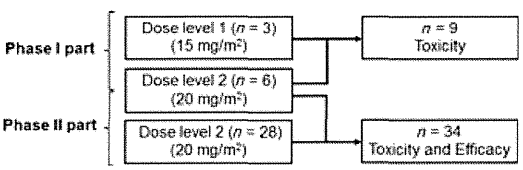

Fig. 1. Study schema. A total of 37 patients were treated in this study. In the phase I part, three received 15 mg/m^2 and six received 20 mg/m^2. In the phase II part, 28 additional patients received 20 mg/m^2. Toxicity was analyzed in all patients. Efficacy was analyzed in all patients who received 20 mg/m^2.

Antiemetics were not routinely given. The use of erythropoietin was not allowed. Granulocyte colony stimulating factor was allowed as clinically indicated, but response was recorded when patients were not receiving growth factor support. Dose reductions of the study drug were not allowed.

Toxicity and response evaluation. Toxicity was evaluated based on Common Terminology Criteria for Adverse Event (CTCAE) version 3.0. DLT was defined as: non-hematologic toxicity $\geq$ grade 3, excluding nausea and vomiting, and neutropenic fever and infection $\geq$ grade 3 that did not improve despite a delay in the initiation of the next cycle of treatment by 2 weeks.

Bone marrow aspiration slides were centrally reviewed and final data analysis was conducted based on central review. Response was evaluated based on International Working Group (IWG) 2000[10] and IWG 2006[11] response criteria in myelodysplasia. Complete cytogenetic response was defined as the disappearance of cytogenetic abnormalities; partial cytogenetic response was defined as a $\geq 50\%$ reduction in cytogenetic abnormalities.[10,11] Response duration was calculated from first evidence of response until disease progression.[10,11] Survival was calculated from start of therapy to death from any cause. Time to AML was calculated from start of therapy to the first date of documented marrow blast percentage $\geq 30\%$.

Statistical considerations. In phase I, three patients were to be accrued at 15 mg/m^2. If DLT was not observed in any patients during the first cycle, six more patients were accrued

Table 1. Baseline characteristics of patients

Patient characteristics	Phase	I		I (n = 6) and II (n = 28)	Total
	Dose	15 mg/m^2	20 mg/m^2	20 mg/m^2	
n		3	6	34	37
Sex	Male	3 (100.0%)	4 (66.7%)	26 (76.5%)	29 (78.4%)
	Female	0	2 (33.3%)	8 (23.5%)	8 (21.6%)
Age	<65	0	3 (50.0%)	10 (29.4%)	10 (27.0%)
	65–74	3 (100.0%)	1 (16.7%)	17 (50.0%)	20 (54.1%)
	>75	0	2 (33.3%)	7 (20.6%)	7 (18.9%)
	Median	68 (67–71)	66.5 (54–77)	69 (52–81)	69 (52–81)
PS	0	1 (33.3%)	5 (83.3%)	22 (64.7%)	23 (62.2%)
	1	2 (66.7%)	1 (16.7%)	12 (35.3%)	14 (37.8%)
Type	De novo	2 (66.7%)	5 (83.3%)	29 (85.3%)	31 (83.8%)
	Secondary	1 (33.3%)	1 (16.7%)	5 (14.7%)	6 (16.2%)
Hb (g/dL)	Median (range)	7.1 (5.4–8.7)	7.6 (7.1–8.5)	8.1 (4.7–15.2)	8.0 (4.7–15.2)
Neu (/μL)	Median (range)	434 (312–1243)	887 (173–1910)	898 (143–7416)	807 (143–7416)
Plt	Median (range)	1.2 (1.1–3.6)	7.6 (3.1–22.4)	5.25 (0.3–74.2)	4.9 (0.3–74.2)
Serum EPO (mU/mL)	Median (range)	594 (132–728)	615.5 (31.6–1840)	369 (1538–13 600)	393 (15.8–13 600)
Time from diagnosis	Median	1.1 (0.1–4.1)	1.1 (0.1–4.2) 5	0.55 (0.1–12.7)	0.6 (0.1–12.7)
Prior chemotherapy for MDS	Yes	0	1 (16.7%)	6 (17.6%)	6 (16.2%)
RBC transfusion dependent	Yes	2	4 (66.7%)	25 (73.5%)	27 (73.0%)
Platelet transfusion dependent	Yes	0	0	5 (14.7%)	5 (13.5%)
Previous G-CSF	Yes	0	1 (16.7%)	1 (2.9%)	1 (2.7%)
Type of MDS and IPSS	*De novo* – Low	0	0	1 (2.9%)	1 (2.7%)
	De novo – Intermediate-1	1 (33.3%)	1 (16.7%)	9 (26.5%)	10 (27.0%)
	De novo – Intermediate-2	0	2 (33.3%)	7 (20.6%)	7 (18.9%)
	De novo – High	0	1 (16.7%)	11 (32.4%)	11 (29.7%)
	Secondary MDS	1 (33.3%)	1 (16.7%)	5 (14.7%)	6 (16.2%)
	AML	1 (33.3%)	1 (16.7%)	1 (2.9%)	2 (5.4%)

EPO, erythropoietin; G-CSF, granulocyte-colony stimulating factor; IPSS, International Prognostic Scoring System; MDS, myelodysplastic syndrome; RBC, red blood cell.

doi: 10.1111/j.1349-7006.2012.02386.x

Table 2. Baseline characteristics of bone marrow

Bone marrow characteristics	Phase	I		I (n = 6) and II (n = 28)	Total
	Dose	15 mg/m^2	20 mg/m^2	20 mg/m^2	
n		3	6	34	37
Marrow Blast percent	<5	0 (0.0%)	4 (66.7%)	12 (35.3%)	12 (32.4%)
	5–10	2 (66.7%)	0 (0.0%)	4 (11.8%)	6 (16.2%)
	11–20	0 (0.0%)	0 (0.0%)	11 (32.4%)	11 (29.7%)
	21–30	0 (0.0%)	1 (16.7%)	6 (17.6%)	6 (16.2%)
	>30	1 (33.3%)	1 (16.7%)	1 (2.9%)	2 (5.4%)
	Median	9.2 (7.4–37.1)	4.2 (2.2–52.5)	11.1 (1.0–52.5)	11 (1–52.5)
Bone marrow cellularity	Hyper	0 (0.0%)	3 (50.0%)	13 (38.2%)	13 (35.1%)
	Normo	1 (33.3%)	2 (33.3%)	9 (26.5%)	10 (27.0%)
	Hypo	2 (66.7%)	1 (16.7%)	12 (35.3%)	14 (37.8%)
FAB classification	RA	0 (0.0%)	3 (50.0%)	11 (32.4%)	11 (29.7%)
	RARS	0 (0.0%)	1 (16.7%)	1 (2.9%)	1 (2.7%)
	RAEB	2 (66.7%)	0 (0.0%)	14 (41.2%)	16 (43.2%)
	RAEB-T	0 (0.0%)	1 (16.7%)	7 (20.6%)	7 (18.9%)
	CMML	0 (0.0%)	0 (0.0%)	0 (0.0%)	0 (0.0%)
	AML	1 (33.3%)	1 (16.7%)	1 (2.9%)	2 (5.4%)
WHO classification	RA	0 (0.0%)	0 (0.0%)	3 (8.8%)	3 (8.1%)
	RARS	0 (0.0%)	0 (0.0%)	0 (0.0%)	0 (0.0%)
	RCMD	0 (0.0%)	3 (50.0%)	7 (20.6%)	7 (18.9%)
	RCMD-RS	0 (0.0%)	1 (16.7%)	1 (2.9%)	1 (2.7%)
	RAEB-1	2 (66.7%)	0 (0.0%)	4 (11.8%)	6 (16.2%)
	RAEB-2	0 (0.0%)	0 (0.0%)	10 (29.4%)	10 (27.0%)
	MDS-U	0 (0.0%)	0 (0.0%)	0 (0.0%)	0 (0.0%)
	Other	0 (0.0%)	0 (0.0%)	1 (2.9%)	1 (2.7%)
	AML	1 (33.3%)	2 (33.3%)	8 (23.5%)	9 (24.3%)
Chromosome	Any chromosome abnormality	1 (33.3%)	2 (33.3%)	17 (50.0%)	18 (48.6%)
	Good	2 (66.7%)	4 (66.7%)	14 (41.2%)	16 (43.2%)
	Intermediate	0 (0.0%)	0 (0.0%)	3 (8.8%)	3 (8.1%)
	Poor	1 (33.3%)	2 (33.3%)	17 (50.0%)	18 (48.6%)
	Chromosome 7	0 (0.0%)	1 (16.7%)	12 (35.3%)	12 (32.4%)
	Complex	1 (33.3%)	2 (33.3%)	12 (35.3%)	13 (35.1%)

AML, acute myelogenous leukemia; CMML, chronic myelomonocytic leukemia; FAB, French-American-British; MDS, myelodysplastic syndrome; RA, refractory anemia; RARS, RA with ringed sideroblasts; RAEB, RA with excess blasts; RAEB-T, RAEB in transformation; RCMD, refractory cytopenia with multilineage dysplasia; RCMD-RS, RCMD with ringed sideroblast; WHO, World Health Organization.

Table 3. Observed toxicities

	Grade	15 mg/m^2 (n = 3)			20 mg/m^2 (n = 34)		
		1 or 2	3	4	1 or 2	3	4
Hematologic	Leukocytopenia	0	0	3 (100%)	2 (5.9%)	9 (26.5%)	23 (67.6%)
	Neutropenia	0	0	3 (100%)	0	2 (5.9%)	25 (73.5%)
	Thrombocytopenia	0	0	3 (100%)	1 (2.9%)	6 (17.6%)	21 (61.8%)
	Anemia	0	1 (33.3%)	2 (66.7%)	1 (2.9%)	13 (38.2%)	16 (47.1%)
	Lymphocytopenia	0	2 (66.7%)	1 (33.3%)	11 (32.4%)	11 (32.4%)	6 (17.6%)
Infection	Febrile neutropenia	0	0	1 (33.3%)*	0	8 (23.5%)	2 (5.9%)*
	Other infection	1 (33.3%)	1 (33.3%)	0	6 (17.6%)	10 (29.4%)	0
General	Insomnia	1 (33.3%)	0	0	0	0	0
	Abdominal pain	1 (33.3%)	0	0	0	0	0
Dermatologic	Erythema multiforme	1 (33.3%)	0	0	0	0	0
Gastrointestinal	Elevated transaminase	1 (33.3%)	0	0	8 (23.5%)	1 (2.9%)	0
	Elevated bilirubin	1 (33.3%)	0	0	0	0	0
	Elevated alkaline phosphatase	1 (33.3%)	0	0	0	0	0
Endocrine	Hyperglycemia	0	0	0	9 (26.5%)	1 (2.9%)	0
Cardiovascular	Cerebral infarction	0	0	0	0	1 (2.9%)	0
	Pulmonary hypertension	0	0	0	0	1 (2.9%)	0
Hemorrhage	Subdural hematoma	0	0	0	0	1 (2.9%)	0

*Including grade 5 pneumonia (n = 1 each).

Table 4. Response to decitabine treatment

	Doses	15 mg/m^2 (n = 3)	20 mg/m^2 (n = 34)	Total (n = 37)
IWG 2000	CR	0 (0.0%)	7 (20.6%)	7 (18.9%)
	PR	1 (33.3%)	2 (5.9%)	3 (8.1%)
	HI	1 (33.3%)	5 (14.7%)	6 (16.2%)
	SD	1 (33.3%)	4 (11.8%)	5 (13.5%)
	PD	0 (0.0%)	3 (8.8%)	3 (8.1%)
	NE	0 (0.0%)	13 (38.2%)	13 (35.1%)
	CR + PR (%, 95% CI)	1 (33.3% [0.8–90.6%])	9 (26.5% [12.9–44.4%])	10 (27.0% [13.8–44.1%])
	CR + PR + HI (%, 95% CI)	2 (66.7% [9.4–99.2%])	14 (41.2% [24.6–59.3%])	16 (43.2% [27.1–60.5%])
IWG2006	CR	0 (0.0%)	7 (20.6%)	7 (18.9%)
	PR	1 (33.3%)	2 (5.9%)	3 (8.1%)
	mCR	1 (33.3%)	1 (2.9%)	2 (5.4%)
	HI	0 (0.0%)	4 (11.8%)	4 (10.8%)
	SD	1 (33.3%)	4 (11.8%)	5 (13.5%)
	PD	0 (0.0%)	3 (8.8%)	3 (8.1%)
	NE	0 (0.0%)	13 (38.2%)	13 (35.1%)
	CR + PR (%, 95% CI)	1 (33.3% [0.8–90.6%])	9 (26.5% [12.9–44.4%])	10 (27.0% [13.8–44.1%])
	CR + PR + mCR (%, 95% CI)	2 (66.7% [9.4–99.2%])	10 (29.4% [15.1–47.5%])	12 (32.4% [18.0–49.8%])
	CR + PR + mCR+HI (%, 95% CI)	2 (66.7% [9.4–99.2%])	14 (41.2% [24.6–59.3%])	16 (43.2% [27.1–60.5%])

CR, complete response; HI, hematologic improvement; mCR, marrow complete response; NE, not evaluated; PD, progressive disease; PR, partial response; SD, stable disease.

at 20 mg/m^2. If the 20 mg/m^2 dose was not associated with DLT, this population was carried into phase II. Based on prior studies (response rate 17–35%[6–8,12]), the expected response rate was 25%. The drug was considered ineffective if the response rate was $\leq$5%. With $\alpha = 0.05$ and $\beta = 0.2$, 21 patients would be required to evaluate drug efficacy. Estimating that up to 20% of patients might be found ineligible after central pathologic review, a total of at least 26 patients (including six patients from phase I study at the same dose) were to be enrolled.

Correlative analysis. *Pharmacokinetics.* Plasma decitabine levels were analyzed on days 1 and 5 of treatment in patients in phase I. Blood was drawn at 0, 30, 60, 65, 75, 90, 120, 180 and 240 min after initiation of infusion. Samples were immediately stored at 4°C, and plasma decitabine concentrations were determined by liquid chromatography coupled with tandem mass spectrometry (lower limit of quantification: 1.0 ng/mL).[13]

Pharmacodynamics. Preparation of patient samples: In phase I, we conducted DNA methylation analysis using peripheral blood samples from all nine patients. Samples were obtained before treatment (at baseline) and on days 5, 12, and 28 of the first cycle of decitabine treatment. Two separate cell populations were obtained from whole blood: peripheral blood mononuclear cells (PBMCs) were isolated with standard ficoll separation of whole blood and CD15-positive peripheral blood cells (CD15 + PBCs) were isolated using CD15-recognizing antibodies (Dynabeads CD15; Life Technologies, Carlsbad, CA, USA). CD15 + PBCs were chosen because it has been shown that the majority of PBMCs are lymphocytes, which may not be representative of myelodysplastic cells.[14] CD15, however, is expressed on myeloid cells, including neutrophils, eosinophils and monocytes, and this selection enriched the myeloid cell population and eliminated lymphocytes.

Bisulfite-pyrosequencing for DNA methylation analysis: DNA methylation levels were quantitatively measured using bisulfite-pyrosequencing[15–17] (Pyrosequencing AB, Uppsala, Sweden) for *PGR*, *ESR1*, *CDH1*, *CDH13*, and *LINE1*. The list of primers for bisulfite-pyrosequencing is provided in Table S1. *LINE1* is a repetitive component that we used as a surrogate for global methylation. The methylation levels at different CpG sites were averaged to represent the degree of methylation.

Methylated CpG island amplification and microarray analysis: The DNA methylation status of CD15 + PBC during the first cycle of treatment was further analyzed with methylated CpG island amplification and microarray (MCAM) technology as previously reported[18] using microarrays from Agilent Technologies, which analyzes 6157 genes.

Results

Study enrollment. In phase I, the first cycle of treatment was not associated with DLT. Therefore, the study was expanded into phase II. Data from 34 patients treated with 20 mg/m^2 decitabine were analyzed for safety and efficacy (Fig. 1). Patient characteristics and disease characteristics are summarized in Tables 1 and 2, respectively. All patients had MDS based on local hemato-morphological review, among whom two were found to have AML upon central review of marrow (blast count $\geq$ 30%).

Treatment delivery. A total of 298 cycles were given to 37 patients. A median of 6.0 (range 1–17) and 5.5 cycles (1–17) were delivered per patient in the whole group (15 and 20 mg/m^2) and 20 mg/m^2 group, respectively. Drug administration was delayed due to cytopenia and/or infection by longer than 7 days (i.e. interval >5 weeks) for 84 cycles (28%). Eight patients experienced DLT within two cycles of treatment and

Table 5. Cytogenetic response in patients who originally had cytogenetic abnormalities

Patient No.	Karyotype	Chromosome abnormality	Cytogenetic response
11	Poor	Chromosome 7 abnormalities, complex	Major/ Complete
16	Poor	Chromosome 7 abnormalities, complex	Major/ Complete
18	Intermediate	Trisomy 8	Major/ Complete
20	Poor	Complex	Major/ Complete
24	Good	20q-	Major/ Complete
25	Poor	Complex	Minor/Partial
28	Poor	Chromosome 7 abnormalities, complex	Major/ Complete

doi: 10.1111/j.1349-7006.2012.02386.x

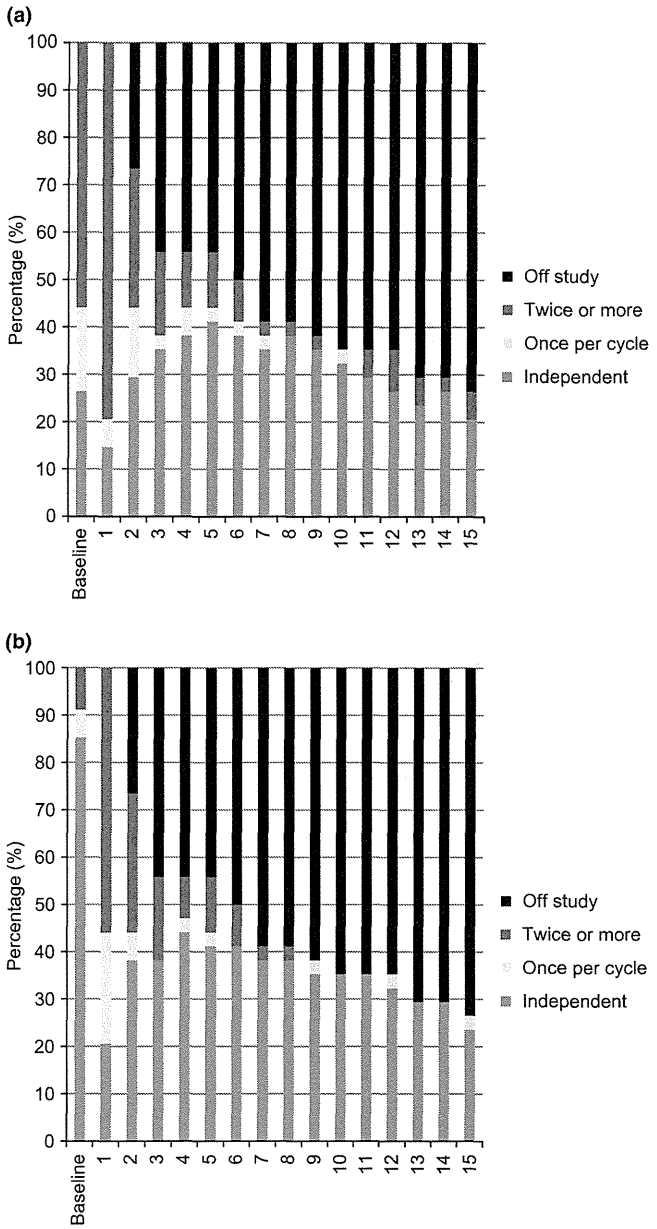

Fig. 2. Transfusion independence. Transfusion independence was calculated using all enrolled patients as the denominator (n = 34). (a) Red cell transfusion independence. The transfusion independence rate increased from 26% (baseline) to 41% after five cycles. (b) Platelet transfusion independence. The color indicates the number of transfusions required per cycle. At baseline 85% of patients were transfusion independent. The majority of patients who continued on treatment past cycle 6 did not require platelet transfusion after that cycle.

did not continue treatment. Reasons for discontinuation included pneumonia associated with neutropenia (n = 5), fungal pneumonia with pulmonary hypertension (n = 1), chronic subdural hematoma (n = 1), and elevated liver enzymes (n = 1). Seven patients were actively receiving decitabine upon trial closure in March 2011 and had received 14–22 cycles of treatment.

Toxicity. Toxicity data are summarized in Table 3. If one patient experienced the same toxicity multiple times, the highest grade is recorded.

15 mg/m^2 group. None of the three patients enrolled in the phase I study experienced DLT during the first cycle of

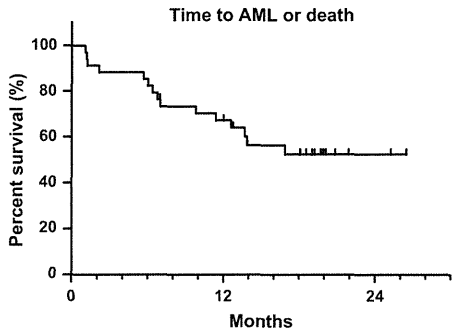

Fig. 3. Time to acute myeloid leukemia or death. Median time to acute myeloid leukemia or death has not been reached. The 2-year rate was 52%.

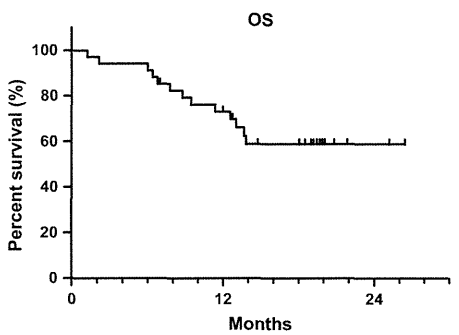

Fig. 4. Overall survival. Median survival has not been reached. The 2-year rate was 56%.

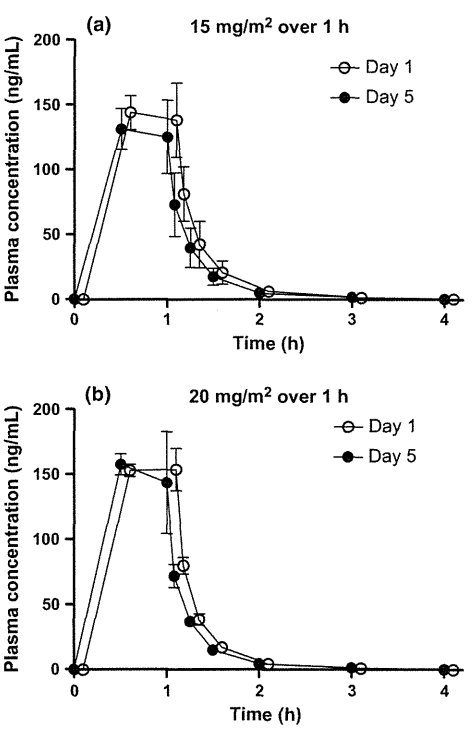

Fig. 5. Plasma concentrations of decitabine – time profile (Mean ± standard error of mean). Mean plasma concentration is plotted with standard error of mean. The data are from: (a) three patients receiving 15 mg/m^2, and (b) five patients receiving 20 mg/m^2 (one patient receiving 20 mg/m^2 in phase I chose not to participate in the pharmacokinetic analysis).

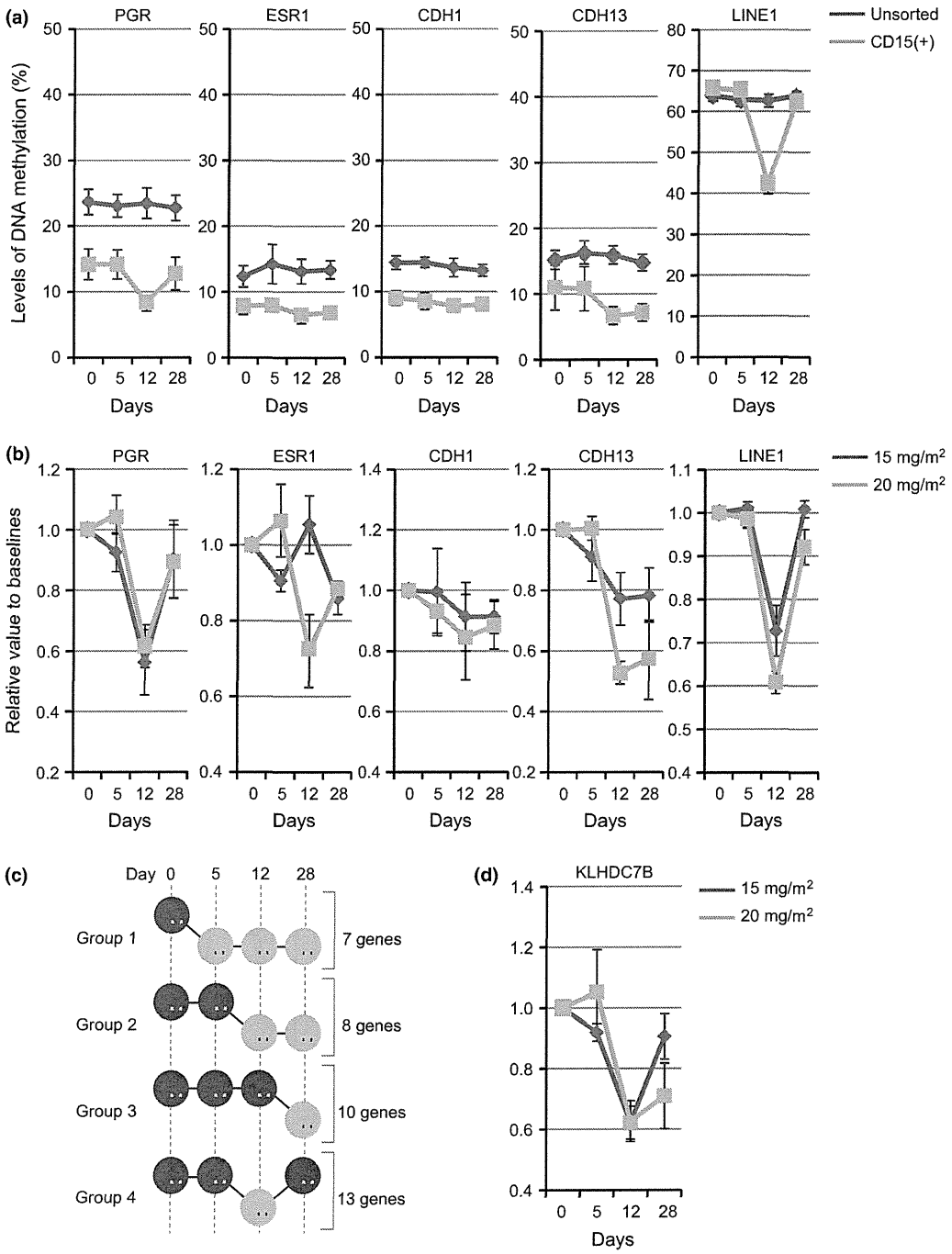

Fig. 6. Changes in the methylation status in five selected genes using peripheral blood mononuclear cells or CD15 + peripheral blood cells (Mean ± standard error of mean). (a) Average methylation changes (0, baseline, and 5, 12 and 28 days after treatment) were compared between peripheral blood mononuclear cells (black lines) and CD15-positive blood cells (gray lines). The *y*-axis shows methylation level (%). (b) Average methylation changes (0, baseline, and 5, 12 and 28 days after treatment) were compared between patients treated with 15 mg/m^2 (black lines) and 20 mg/m^2 (gray lines). The *y*-axis shows relative changes to methylation levels at baseline. (c) DNA demethylation status after decitabine treatment was classified into four groups. (d) Genes in Group 4 show prominent demethylation around 12 days after decitabine treatment. Methylation status of a representative newly identified gene, KLHDC7B, is shown. Methylation changes (at 0, baseline, and 5, 12 and 28 days after treatment) were compared between patients treated with 15 mg/m^2 (black lines) and 20 mg/m^2 (gray lines). The *y*-axis shows relative changes compared to methylation levels at baseline.

treatment, and all continued treatment at this dose. All three patients experienced grade 3 or 4 hematologic toxicities and all received granulocyte-colony stimulating factor (G-CSF). One patient developed pneumonia on day 20 of the 9th course, which progressed rapidly, and this patient died 10 days later. There were no other severe non-hematologic toxicities reported.

20 mg/m^2 group. Thirty-four patients received the 20 mg/m^2 dose. As shown in Table 3, myelosuppression was very common, a similar finding to that of previous studies. A total of 17

doi: 10.1111/j.1349-7006.2012.02386.x

Table 6. Summary of large studies of decitabine and azacitidine

Study	Phase	Drug	Dose	Outcome
CALGB[24]	III	Azacitidine	Best supportive care (n = 92)	CR 0%, PR 0% (IWG2000)
			Crossover allowed	Median OS 14 months
			75 mg/m^2 per day × 7 days (n = 99)	CR 6.1%, PR 10.1%
			CR + 2 more cycles	Median OS 20 months (P = 0.10)
				A land mark analysis eliminating the effect of cross over showed benefit of azacitidine P = 0.03
International[23]	III	Azacitidine	Physician's choice (n = 179)	CR rate 16% (IWG2000)
				Median OS 15.0 months
			75 mg/m^2 per day × 7 days (n = 179)	CR rate 18% (P = 0.80)
			At least four cycles	Median OS 24.4 months (P < 0.01)
US multi institutional[6]	III	Decitabine	Best supportive care (n = 81)	CR 0%, PR 0% (IWG2000)
				Median leukemia free survival 7.8 months
			15 mg/m^2 Q 8 h, nine doses (n = 89)	CR 9%, PR 8%
			Max eight cycles	Median leukemia free survival 12.1 months (P = 0.16)
EORTC[12]	III	Decitabine	Best supportive care (n = 114)	CR 0%, PR 0% (IWG2000)
				Median OS 8.5 months
			15 mg/m^2 Q 8 h, nine doses (n = 119)	CR 13%, PR 6%
			Max eight cycles	Median OS 10.1 months (P = 0.38)
MDACC[7]	II	Decitabine	20 mg/m^2 daily for 5 days and two other arms 100 mg/m^2 per course (n = 95)	CR 34%, mCR 24%, PR 1%, HI 13% (IWG2006)
				Median OS 19 months
ADOPT[8]	II	Decitabine	20 mg/m^2 daily for 5 days (n = 99)	CR 17%, mCR 15%, PR 0%, HI 18% (IWG2006)
				Median OS 19.4%
Japanese Azacitidine	II	Azacitidine	75 mg/m^2 per day × 7 days (n = 53)	CR 15%, mCR 13%, PR 0%, HI 55% (IWG2006)
Our study	II	Decitabine	20 mg/m^2 daily for 5 days (n = 34)	CR 21%, mCR 3%, PR 6% (IWG2006)
				Median OS not reached

ADOPT, Alternative Dosing for Outpatient Treatment Trial; CALGB, Cancer and Leukemia Group B; CR, complete remission; EORTC, European Organization for Research and Treatment of Cancer; HI, hematologic improvement; IWG, Response criteria by International Working Group; mCR, marrow complete remission; MDACC, MD Anderson Cancer Center; OS, overall survival; PR, partial remission.

patients received G-CSF. One patient experienced prolonged grade 4 neutropenia and was taken off the study. Another patient developed pneumonia on day 13 of cycle 2 and died 3 weeks later. Non-hematologic toxicities ≥ grade 3 included cerebral infarction (n = 1, grade 3), subdural hematoma (n = 1, grade 3), elevated blood glucose (n = 1, grade 3), and pulmonary hypertension (n = 1, grade 3).

Response. Response data are summarized in Table 4. Out of 37 patients, CR, PR and hematologic improvement (HI) defined by IWG2000 criteria were observed in 7 (18.9%), 3 (8.1%) and 6 (16.2%), respectively. By IWG2006 criteria, CR, PR, marrow CR and HI were observed in 7 (18.9%), 3 (8.1%) and 2 (5.4%) and 4 (10.8%), respectively. When analysis was limited to the 34 patients who received treatment at 20 mg/m^2, CR and PR were observed in 7 (20.6%) and 2 (5.9%), respectively, both by IWG2000 and IWG2006 criteria. In patients who achieved response (CR + PR, n = 9) at 20 mg/m^2, median time to remission was 130 days (range 67–220), or four cycles (range 4–8), and duration of remission was 474+ days (range 294–598+).

When the analysis was limited to patients with marrow blast percentage <20% (n = 28), the CR rate was 17.9% and CR + PR rate was 25.0% by both IWG2000 and IWG2006 criteria (Table S1).

Cytogenetic response was evaluable in 20 patients who had karyotype abnormalities upon study entry. Six patients (30%) achieved complete cytogenetic response, while one patient (5%) achieved partial cytogenetic response. Cytogenetic changes are shown in detail in Table 5.

Transfusion independence. Transfusion independence over time is shown in Figure 2. Percentages were calculated using all enrolled patients as the denominator (n = 34).

Red cell transfusion independence. At baseline, 26% of patients were red cell transfusion-independent. Although this number decreased to 15% of patients after the first cycle, it increased again after two cycles, hitting a peak of 41% after five cycles. Transfusion independence decreased again after 10 cycles, but many who were transfusion-independent continued treatment. Details are shown in Figure 2(a).

Platelet transfusion independence. At baseline, 85% of patients were platelet transfusion-independent, with that number falling to 21% after the first cycle. However, transfusion independence increased as patients continued on treatment, and most patients who were able to continue treatment through cycle 6 became platelet transfusion-independent after that cycle. Details are shown in Figure 2(b).

Time to acute myelogenous leukemia or death and overall survival. Kaplan–Meier estimates of time to AML or death are plotted in Figure 3. Median time to AML or death has not been reached. The 2-year rate of AML-free survival is 52%. Kaplan–Meier estimates of overall survival are shown in Figure 4. Median survival has not been reached. The 2-year survival rate is 56%. These data are comparable to previously reported data in similar patient populations receiving the same treatment in the United States and Europe.[6–8]

Pharmacokinetics. Plasma concentrations of decitabine were analyzed on days 1 and 5 in three patients receiving 15 mg/m^2 and five patients receiving 20 mg/m^2 (Fig. 5). Plasma decitabine became undetectable within 240 min. No significant difference in plasma decitabine concentrations between days 1 and 5 was observed. In addition, plasma levels at each time point and the calculated area under the curve were not apparently different between the 15 and 20 mg/m^2 groups (data not shown), although this could be due to the limited number of evaluable subjects and considerable individual variation.

Pharmacodynamics. *Changes in DNA methylation in peripheral blood mononuclear cells and CD15 + peripheral blood cells.* Changes in methylation of five selected genes in PBMCs and CD15 + PBCs are summarized in Figure 6(a). In general,

the degree of methylation at baseline was higher in PBMCs than in CD15 + PBCs, although the difference was not statistically significant. Average baseline methylation in PBMCs and CD15 + PBCs was 24% and 14%, respectively, for *PGR* ($P = 0.007$), 12% and 8% for *ESR1* ($P = 0.03$), 14% and 9% for *CDH1* ($P = 0.002$), and 15% and 11% for *CDH13* ($P = 0.28$). The hypomethylating effect of decitabine seemed most prominent on day 12, and was more prominent in CD15 + PBCs than in PBMCs, particularly in *LINE1* ($P < 0.0001$). With this result, and given that CD15 + PBCs represent affected myeloid cells more accurately than PBMCs, we chose to analyze the DNA methylation status of CD15 + PBCs. Changes in methylation status after treatment were more prominent in patients receiving 20 mg/m^2 than in those receiving 15 mg/m^2 (Fig. 6b).

Methylated CpG island amplification and microarray analysis. A variable number of genes were found to be methylated at baseline (average: 548 genes; range: 140–1029 genes) after genome-wide DNA methylation profiling using MCAM.[19] While a majority of these genes sustained detectable levels of DNA methylation after decitabine treatment, 25 genes showed significant hypomethylation. Persistent hypomethylation was observed starting on day 5 (Group 1), day 12 (Group 2), and day 28 (Group 3) in seven, eight, and 10 genes, respectively (Fig. 6c, Table S3). Notably, prominent hypomethylation on day 12 followed by recovery of methylation, as observed most dramatically in *LINE1*, was observed in 13 genes (Group 4). Thus, 21 genes (55%) showed prominent DNA demethylation on day 12. Using MCAM analysis, we identified a kelch domain-containing protein, 7B (KLHDC7B), which warrants further investigation as a surrogate marker for demethylation after decitabine treatment (Fig. 6d). As we did not observe major clinical response in phase I, correlation between methylation and clinical outcome could not be analyzed.

Discussion

Decitabine was well tolerated and induced durable response in this Japanese population. Decitabine has previously been investigated in multiple clinical trials (Table 6). The treatment regimen studied here was investigated in a phase II study at MD Anderson[20] and in a multi-institutional study.[8] Compared to treatment with 15 mg/m^2 over 3 h every 8 h for 3 days, treatment with 20 mg/m^2 over 1 h daily for 5 days is more convenient, can be given in an outpatient setting and has comparable efficacy.

The only grade 3/4 toxicities observed in >10% of patients were hematologic and infectious toxicities, which are characteristic of the disease itself, although treatment with decitabine certainly requires careful blood count monitoring and infection surveillance. Overall, the observed toxicity profile was comparable to that of azacitidine reported in a phase I/II study conducted in Japan.[21] In particular, the incidences of grade 3/4 febrile neutropenia in the present study and the Japanese azacitidine study were similar at 29.4% and 30.2%, respectively.[21]

Randomized phase III studies of decitabine versus best supportive care have not shown significant survival benefit for decitabine.[6,12] This could be due to the fact that decitabine at 15 mg/m^2 over 3 h every 8 h for 3 days, not the dose and schedule studied here, was used in the US and European Organization for Research and Treatment of Cancer (EORTC) studies. In addition, only a limited percentage of patients in these studies continued treatment after experiencing clinical benefit.[6,12] Continuation of treatment in patients who are responding is beneficial, but previous randomized phase III studies set a maximum number of treatment cycles, which affected responders in particular.

There are several differences in the mechanisms of action of azacitidine and decitabine. First, azacitidine is a ribose-based nucleoside and is mostly incorporated into RNA. A small proportion of azacitidine diphosphate is reduced by ribonucleotide reductase to decitabine diphosphate and is eventually incorporated into DNA, which can result in the inhibition of DNA methyltransferase. In contrast, decitabine is incorporated into DNA after phosphorylation and does not require reduction. Second, azacitidine is incorporated into RNA and inhibits DNMT2. This can inhibit methylation of tRNA(Asp)-cytosine 38 and may exert toxicity.[22] Decitabine does not have this effect. Finally, the mechanisms of resistance may be different, as illustrated by the difference in the rate-determining step of phosphorylation of each; deoxycytidine kinase limits the rate of phosphorylation for decitabine while uridine-cytidine kinase limits that of azacitidine. Decreases in the expression or activity of these enzymes may be associated with drug resistance, and thus certain cells may be more sensitive to one drug than the other.

Our study confirmed that hypomethylation is observed after decitabine therapy. Robust methylation analysis also revealed that certain sets of genes were hypomethylated after decitabine therapy, although the significance of these changes should be further evaluated. In this study, methylation status in CD15 + PBCs, rather than PBMCs, was analyzed for the first time. The changes in methylation were generally more prominent in CD15 + PBSs than in PBMCs. As this cell population better reflects myeloid cell behavior, we propose this method be used in future analysis of *in vivo* methylation changes in patients treated with a hypomethylating agent.

In summary, our study has shown the safety and clinical activity of decitabine in Japanese patients with high-risk MDS. Responses and toxicities are comparable to those reported in previous studies. Correlative analysis revealed hypomethylation in a number of genes *in vivo* after decitabine treatment, which warrants further investigation in the setting of epigenetic therapy.

Acknowledgments

We thank all the patients and families who participated in this trial. We also thank all institutional investigators and their clinical research staff. This study was supported by Janssen Pharmaceutical K.K.

Disclosure Statement

Y. Kobayashi and M. Ogura have received a consultant fee from Janssen Pharmaceutical KK. The other authors reported no conflicts of interest.

References

1 Garcia-Manero G. Myelodysplastic syndromes: 2011 update on diagnosis, risk-stratification, and management. *Am J Hematol* 2011; **86**: 490–8.
2 Greenberg P, Cox C, LeBeau MM *et al.* International scoring system for evaluating prognosis in myelodysplastic syndromes. *Blood* 1997; **89**: 2079–88.
3 Jones PA, Baylin SB. The fundamental role of epigenetic events in cancer. *Nat Rev Genet* 2002; **3**: 415–28.
4 Shen L, Kantarjian H, Guo Y *et al.* DNA methylation predicts survival and response to therapy in patients with myelodysplastic syndromes. *J Clin Oncol* 2010; **28**: 605–13.
5 Kaminskas E, Farrell A, Abraham S *et al.* Approval summary: azacitidine for treatment of myelodysplastic syndrome subtypes. *Clin Cancer Res* 2005; **11**: 3604–8.

doi: 10.1111/j.1349-7006.2012.02386.x

6 Kantarjian H, Issa JP, Rosenfeld CS *et al.* Decitabine improves patient outcomes in myelodysplastic syndromes: results of a phase III randomized study. *Cancer* 2006; **106**: 1794–803.
7 Kantarjian H, Oki Y, Garcia-Manero G *et al.* Results of a randomized study of 3 schedules of low-dose decitabine in higher-risk myelodysplastic syndrome and chronic myelomonocytic leukemia. *Blood* 2007; **109**: 52–7.
8 Steensma DP, Baer MR, Slack JL *et al.* Multicenter study of decitabine administered daily for 5 days every 4 weeks to adults with myelodysplastic syndromes: the alternative dosing for outpatient treatment (ADOPT) trial. *J Clin Oncol* 2009; **27**: 3842–8.
9 Lee JH, Jang JH, Park J *et al.* A prospective multicenter observational study of decitabine treatment in Korean patients with myelodysplastic syndrome. *Haematologica* 2011; **96**: 1441–7.
10 Cheson BD, Bennett JM, Kantarjian H *et al.* Report of an international working group to standardize response criteria for myelodysplastic syndromes. *Blood* 2000; **96**: 3671–4.
11 Cheson BD, Greenberg PL, Bennett JM *et al.* Clinical application and proposal for modification of the International Working Group (IWG) response criteria in myelodysplasia. *Blood* 2006; **108**: 419–25.
12 Lubbert M, Suciu S, Baila L *et al.* Low-dose decitabine versus best supportive care in elderly patients with intermediate- or high-risk myelodysplastic syndrome (MDS) ineligible for intensive chemotherapy: final results of the randomized phase III study of the European Organisation for Research and Treatment of Cancer Leukemia Group and the German MDS Study Group. *J Clin Oncol* 2011; **29**: 1987–96.
13 Cashen AF, Shah AK, Todt L *et al.* Pharmacokinetics of decitabine administered as a 3-h infusion to patients with acute myeloid leukemia (AML) or myelodysplastic syndrome (MDS). *Cancer Chemother Pharmacol* 2008; **61**: 759–66.
14 Raza A, Raza FZ, Galili N. Low-dose decitabine and high-risk MDS. *Blood* 2006; **108**: 4291.
15 Gao W, Kondo Y, Shen L *et al.* Variable DNA methylation patterns associated with progression of disease in hepatocellular carcinomas. *Carcinogenesis* 2008; **29**: 1901–10.
16 Colella S, Shen L, Baggerly KA *et al.* Sensitive and quantitative universal Pyrosequencing methylation analysis of CpG sites. *Biotechniques* 2003; **35**: 146–50.
17 Yang AS, Estecio MR, Doshi K *et al.* A simple method for estimating global DNA methylation using bisulfite PCR of repetitive DNA elements. *Nucleic Acids Res* 2004; **32**: e38.
18 Estecio MR, Gallegos J, Vallot C *et al.* Genome architecture marked by retrotransposons modulates predisposition to DNA methylation in cancer. *Genome Res* 2010; **20**: 1369–82.
19 Estecio MR, Yan PS, Ibrahim AE *et al.* High-throughput methylation profiling by MCA coupled to CpG island microarray. *Genome Res* 2007; **17**: 1529–36.
20 Kantarjian HM, O'Brien S, Cortes J *et al.* Results of decitabine (5-aza-2′deoxycytidine) therapy in 130 patients with chronic myelogenous leukemia. *Cancer* 2003; **98**: 522–8.
21 Uchida T, Ogawa Y, Kobayashi Y *et al.* Phase I and II study of azacitidine in Japanese patients with myelodysplastic syndromes. *Cancer Sci* 2011; **102**: 1680–6.
22 Schaefer M, Hagemann S, Hanna K, Lyko F. Azacytidine inhibits RNA methylation at DNMT2 target sites in human cancer cell lines. *Cancer Res* 2009; **69**: 8127–32.
23 Fenaux P, Mufti GJ, Hellstrom-Lindberg E *et al.* Efficacy of azacitidine compared with that of conventional care regimens in the treatment of higher-risk myelodysplastic syndromes: a randomised, open-label, phase III study. *Lancet Oncol* 2009; **10**: 223–32.
24 Silverman LR, Demakos EP, Peterson BL *et al.* Randomized controlled trial of azacitidine in patients with the myelodysplastic syndrome: a study of the cancer and leukemia group B. *J Clin Oncol* 2002; **20**: 2429–40.

Supporting Information

Additional Supporting Information may be found in the online version of this article:

Table S1. List of the primers for bisulfite pyrosequencing analysis.

Table S2. Response to decitabine treatment in patients whose marrow blast was <20%.

Table S3. List of hypomethylated genes in response to decitabine treatment.

Please note: Wiley-Blackwell are not responsible for the content or functionality of any supporting materials supplied by the authors. Any queries (other than missing material) should be directed to the corresponding author for the article.

Molecular Cell
Article

Poly-ADP Ribosylation of Miki by tankyrase-1 Promotes Centrosome Maturation

Yuko Ozaki,[1,7] Hirotaka Matsui,[1,7] Hiroya Asou,[1] Akiko Nagamachi,[1] Daisuke Aki,[1] Hiroaki Honda,[2] Shin'ichiro Yasunaga,[3] Yoshihiro Takihara,[3] Tadashi Yamamoto,[4,5] Shunsuke Izumi,[6] Miho Ohsugi,[4] and Toshiya Inaba[1,*]
[1]Department of Molecular Oncology and Leukemia Program Project
[2]Department of Disease Model
[3]Department of Stem Cell Biology
Research Institute for Radiation Biology and Medicine, Hiroshima University, Hiroshima 734-8553, Japan
[4]Division of Oncology, Institute of Medical Science, University of Tokyo, Tokyo 108-8639, Japan
[5]Cell Signal Unit, Okinawa Institute of Science and Technology, Onna-son, Okinawa 904-0412, Japan
[6]Graduate School of Science, Hiroshima University, Higashihiroshima 739-8511, Japan
[7]These authors contributed equally to this work
*Correspondence: tinaba@hiroshima-u.ac.jp
http://dx.doi.org/10.1016/j.molcel.2012.06.033

SUMMARY

During prometaphase, dense microtubule nucleation sites at centrosomes form robust spindles that align chromosomes promptly. Failure of centrosome maturation leaves chromosomes scattered, as seen routinely in cancer cells, including myelodysplastic syndrome (MDS). We previously reported that the *Miki* (*LOC253012*) gene is frequently deleted in MDS patients, and that low levels of Miki are associated with abnormal mitosis. Here we demonstrate that Miki localizes to the Golgi apparatus and is poly(ADP-ribosyl)ated by tankyrase-1 during late G2 and prophase. PARsylated Miki then translocates to mitotic centrosomes and anchors CG-NAP, a large scaffold protein of the γ-tubulin ring complex. Due to impairment of microtubule aster formation, cells in which tankyrase-1, Miki, or CG-NAP expression is downregulated all show prometaphase disturbances, including scattered and lagging chromosomes. Our data suggest that PARsylation of Miki by tankyrase-1 is a key initial event promoting prometaphase.

INTRODUCTION

Prometaphase is the phase of mitosis when robust mitotic spindles move chromosomes toward the center of the cell and align them on the metaphase plate. If the mechanism(s) promoting progression of prometaphase is impaired, chromosomes are left scattered for an extended period. One example of this is the downregulation of tankyrase-1, one of 18 mammalian poly(ADP-ribose) polymerases (PARPs), which results in severe mitotic defects in prometaphase such as preanaphase arrest, chromosome scattering, and "pseudometaphase" (several lagging chromosomes juxtaposed to, or even behind, spindle poles during metaphase chromosome alignment) (Chang et al., 2005a, 2005b). More recently, downregulation of ch-TOG/XMAP215, a microtubule-processing polymerase that "surfs" on growing microtubule plus ends, was reported to delay prometaphase and to induce pseudometaphase phenotypes (Brouhard et al., 2008; Gergely et al., 2003).

Chromosome scattering and pseudometaphase phenotypes are seen routinely in certain cancer cells, but the molecular mechanisms underlying these abnormalities are largely unknown (Nigg, 2002). Myelodysplastic syndrome (MDS), a common hematopoietic disease previously termed "preleukemia," is one such disease showing abnormal mitoses including so-called colchicine-mitosis (chaotic chromosome scattering similar to colchicine-treated cells) or lagging chromosomes, and subsequent abnormal nuclear morphologies, such as multinucleated cells with micronuclei.

We recently identified a common microdeletion cluster in the long arm of chromosome 7 (Asou et al., 2009), which is a region well known to be frequently deleted in MDS cells (Mauritzson et al., 2002). This microdeletion cluster contains three contiguous genes, *Samd9*, *Samd9L*, and *LOC253012*, each encoding a different product with few known functional motifs. Orthologs of these three genes are found only in vertebrate genomes, and not in invertebrates, plants, yeast, or prokaryotes.

The *Samd9* and *Samd9L* genes result from duplication of a common ancestral gene. Downregulation of Samd9 has also been reported in aggressive fibromatosis (Li et al., 2007). In addition, we recently observed that *Samd9L*-deficient mice develop myeloid malignancies at high frequency (our unpublished data), suggesting that Samd9 and Samd9L are tumor suppressors.

The LOC253012 gene product that we named Miki (mitotic kinetics regulator) translocates from the Golgi apparatus to mitotic centrosomes/spindles in late G2/M phase. Downregulation of this gene in HeLa cells induces prometaphase delay or arrest, with deeply disturbed chromosome alignment including chromosome scattering; pseudometaphase; and consequent bi-, tri-, or multinucleated cells with micronuclei. Intriguingly, Miki expression levels in MDS cells are associated with the abnormal mitosis and nuclear morphology that characterize MDS (Asou et al., 2009).

Here we focus on the function of Miki in mitosis. We demonstrate that Miki is a substrate for tankyrase-1. In late G2 to prophase, tankyrase-1 and PARsylated Miki translocate from the Golgi apparatus to mitotic centrosomes and play critical roles in the formation of robust microtubules for prompt movement of chromosomes.

RESULTS

Localization of Miki to Mitotic Spindles/Centrosomes

Miki (LOC253012 gene product) contains three domains suggestive of a cell surface protein, namely an N-terminal putative signal peptide, a central region with homology to immunoglobulin superfamily cell adhesion molecules (IgCAM), and an extremely hydrophobic transmembrane (TM) domain-like region (Figure 1A).

Unexpectedly, immunostaining of HeLa cells using antibodies against the C terminus of Miki showed an intense signal in the perinuclear region that colocalized with *trans*-Golgi markers such as p230 during interphase (Figure 1B, upper panels), as we previously reported (Asou et al., 2009). Localization of Miki in the Golgi apparatus was confirmed by FLAG immunostaining of HeLa cells expressing C-terminal FLAG-tagged full-length Miki (Miki-FLAG) protein transfected by the MSCV pantropic retrovirus (Figure 1C, middle panels). In contrast, only a small amount of a Miki(ΔN)-FLAG mutant lacking 30 N-terminal amino acids accumulated in the Golgi body (lower panels).

Although Miki does not appear to accumulate in centrosomes during interphase (Figure 1B, lower panels, insets), Miki immunostaining localizes to centrosomes and spindles during prophase, prometaphase, and metaphase of mitosis, and to midbodies at telophase (Figure 1D). Miki-FLAG protein was also detected in mitotic spindles and centrosomes by FLAG antibody (Figure 1E). However, the lack of putative signal peptide greatly reduced the accumulation of Miki(ΔN)-FLAG protein at spindle poles.

Because the antibodies we raised to detect endogenous Miki expression by immunoblotting did not unequivocally detect Miki protein in whole-cell extracts (Asou et al., 2009), we attempted to detect it in extracts from isolated mitotic spindles/centrosomes using a published method (Sillje and Nigg, 2006). Immunoblotting of lysates extracted from isolated mitotic spindles/centrosomes (Figure 1F) showed a band of ~50 kDa, corresponding to the predicted molecular weight of Miki (50.1 kDa), as well as an additional intense large band of ~125 kDa (Figure 1G), which comigrates with a G2/M phase-dominant band detected in whole-cell extracts (see Figure S1 online).

A large protein of ~125 kDa was also detected in immunoprecipitated products of HeLa cells using Miki antibody (Figure 1H, lane 5, arrowhead). We used MALDI-TOF spectroscopy to verify the identity of the immunoprecipitated p125 protein, and peptide mass fingerprinting to determine the molecular weights of the nine peaks resulting from the 125 kDa band. These were found to match the specific masses of Miki tryptic peptide fragments (Figure 1I). Mass spectrometric sequencing of these peaks confirmed that they matched Miki peptide sequences. These data suggest that $p125^{Miki}$ is present in mitotic centrosomes/spindles.

Prometaphase Arrest Resulting in Apoptosis Caused by Miki Downregulation

We previously selected two short-interfering (si) RNAs (siRNA#79 and siRNA#80; Asou et al., 2009) that effectively downregulate Miki expression in HeLa cells (Figure 2A). Upon treatment of HeLa cells with siRNA#80 (100 nM) for 48 hr, the number of floating mitotic cells significantly ($p < 0.01$) increased from 6.1% (control siRNA-treated cells) to 24.3% (siRNA#80-treated cells), suggesting that Miki downregulation disturbs mitosis. Indeed, in mitotic cells treated with siRNA#80 and stained with Hoechst 33342, we frequently observed more than three lagging chromosomes juxtaposed to, or even situated behind, spindle poles during metaphase chromosome alignment (Figure 2B, panel 1, arrows). This is similar to the "pseudometaphase" condition defined by others (Weaver et al., 2003), which is distinct from normal late prometaphase, when less than two (typically only one) lagging chromosomes are located near aligned chromosomes (panel 2, arrow). Mixed mitotic cell (MMC) culture that allows comparison of immunofluorescence signals from mitotic cells treated with different siRNAs (see the Experimental Procedures) revealed that cells with pseudometaphase phenotypes (panels 3 and 4, right-hand cell) showed markedly reduced Miki immunofluorescence signals compared with cells at metaphase (left-hand cell).

Pseudometaphase was observed in 6.7%–18.5% of mitotic cells treated with different concentrations of either siRNA#79 or siRNA#80 (Figure 2C). In contrast, cells treated with control siRNA (200 nM) rarely (<1%) showed pseudometaphase. In addition, a significant increase in telophase cells was also observed in cells treated with siRNA#79 (200 nM) and siRNA#80 (50 nM).

We established U2OS cells constitutively expressing a histone H2B-GFP fusion protein (Ozaki et al., 2011; Shi and King, 2005) and acquired time-lapse images following transfection with siRNAs (efficiency typically 80%). When cells were treated with control siRNA (100 nM) for 36 hr, ~90% of prophase U2OS cells entered anaphase within 45 min (Figure 2D). Early prometaphase in these cells is very short (Movie S1), and within 10 min, most chromosomes were aligned, with few lagging chromosomes near the metaphase plate. In contrast, treatment of cells with siRNA#80 (100 nM) for 36 hr resulted in only 24% of prophase cells entering anaphase within 45 min, and 28% of prophasic cells with prolonged prometaphase (typically around 90 min) (Figure 2D). The rest of the prophasic cells (48%) did not enter anaphase during the 12 hr observation period (Movie S2). In these prometaphase cells, chromosomes appeared to be scattered widely and randomly. Thereafter, the majority of chromosomes lined up transiently at the metaphase plate, but there were a few that did not. Occasionally, scattered chromosomes appeared to rotate synchronously around the cell center, suggesting highly motile spindle poles. Time-lapse observations of U2OS cells expressing a GFP-α-tubulin fusion protein confirmed the rotation of the spindles (Movie S3).

During a 12 hr observation period 36 hr after transfection of siRNA#80, 36% of the transfected cells underwent cell death (Figure 2D, Movie S4). Consistent with this, cells treated with siRNA#80 showed a significant increase in the numbers of annexin V- or TUNEL-positive cells, as well as cells with high

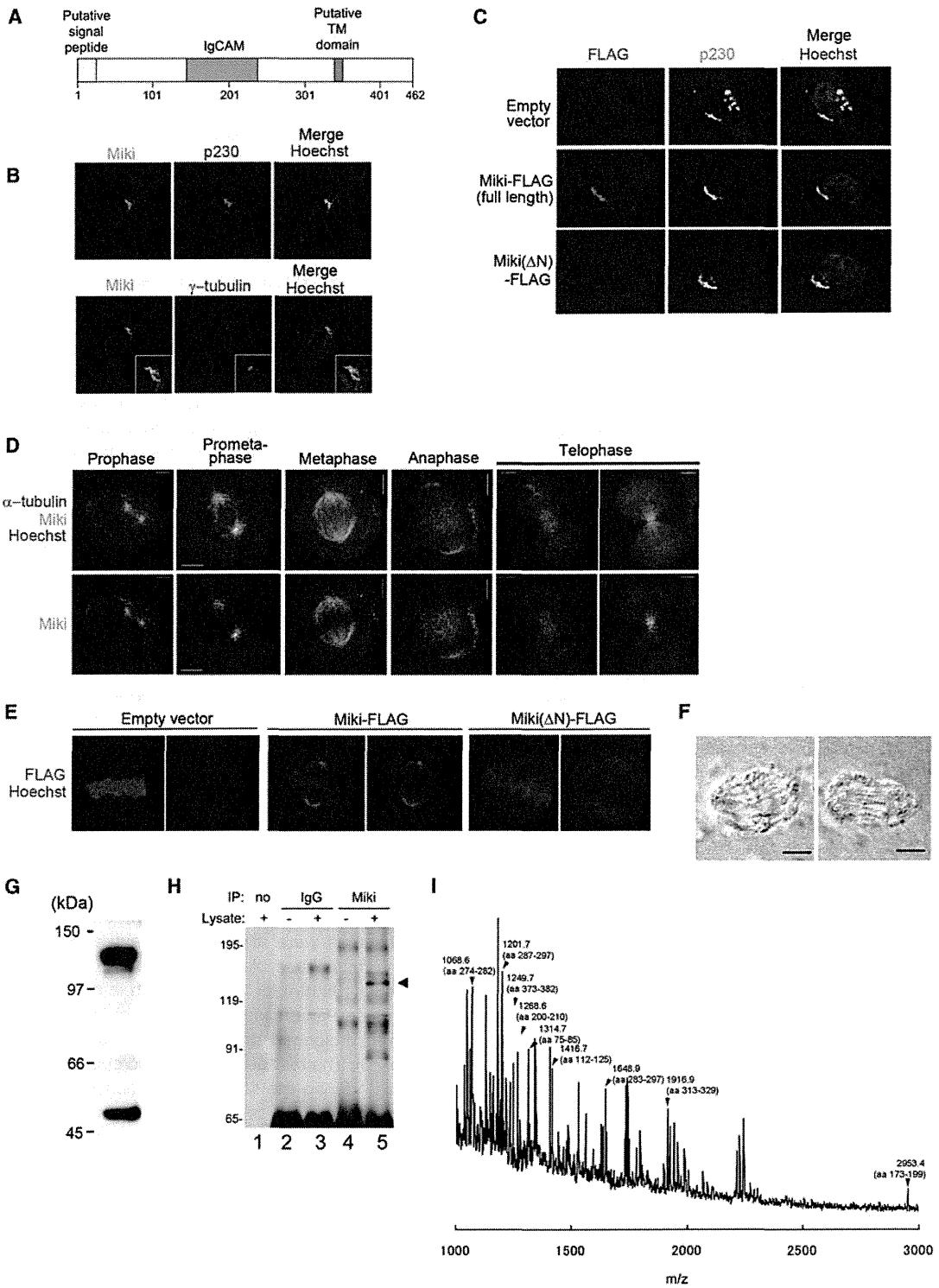

Figure 1. Detection of Miki

(A) Putative functional domains of Miki protein.

(B–E) Immunostaining of HeLa cells in interphase (B and C) or mitosis (D and E) with antibodies indicated above (B and C) or at left (D and E). Nuclear DNA was stained with Hoechst 33342. Insets show enlargements of a centrosomal area (B).

(F) Differential interference contrast (DIC) light microscopy image of isolated mitotic spindles. Scale bar, 5 μm.

caspase-3 activity relative to control untreated cells or cells treated with Miki siRNA#81 (Figure 2E, Figure S2), which does not interfere with Miki mRNA expression (Asou et al., 2009). These data demonstrate that Miki downregulation results in prometaphase delay or arrest, followed by subsequent initiation of apoptosis.

Another subset of cells treated with siRNA#80 showed chromosome decondensation and exit from mitosis in the absence of chromosome segregation (Figure 2F, arrow 1). This resulted in the accumulation of cells containing multiple nuclei of various sizes (arrow 2; arrow 3 shows a normal interphasic nucleus). Together with the overall increase in binucleated cells following Miki downregulation by constitutive expression of short-hairpin RNA (Asou et al., 2009), these observations suggest that Miki downregulation induces abnormal nuclear morphology and long-term chromosomal instability.

To test whether exogenously expressed Miki rescues the pseudometaphase phenotype induced by siRNA#80, HeLa cells were infected with either MSCV/ires-CD8 (an empty pantropic retrovirus) or MSCV-Miki^{MT80}/ires-CD8 (Miki^{MT80} contains the full-length Miki cDNA harboring silent mutations in the target sequence of siRNA#80). CD8-positive cells were then sorted with magnetic beads. Immunoblotting revealed that treatment of cells expressing Miki^{MT80} with siRNA#79 (with a target sequence conserved in Miki^{MT80}) reduced p125^{Miki} and *n*-glycosylated exogenously expressed Miki (Asou et al., 2009) to less than 20% of the amount found in untreated cells or cells treated with control siRNA (Figure 2G, lane 4), while treatment with siRNA#80 decreased p125^{Miki} by only 25% (lane 5). Treatment of control cells (infected with empty retrovirus) or cells expressing Miki^{MT80} with control siRNA did not induce pseudometaphase (Figure 2H). Treatment with siRNA#79 induced a significant increase of cells in pseudometaphase in both controls and cells expressing Miki^{MT80}. Similar changes were also observed in siRNA#80-treated control cells, but not in siRNA#80-treated cells expressing Miki^{MT80}, indicating that exogenous Miki aligns chromosomes promptly.

PARsylation of Miki by tankyrase-1 during Late G2/M Phase

Recent studies indicate that poly(ADP-ribose) (PAR) is enriched in vertebrate mitotic spindles and is required for spindle assembly and function (Chang et al., 2004). PAR perturbation by PAR glycohydrolase (PARG) or anti-PAR antibody results in rapid loss of spindle structure in *Xenopus* eggs. Indeed, in HeLa cells, immunoblotting of isolated mitotic spindles (Figure 1F) with PAR antibody showed marked accumulation of PAR (Figure 3A, lane 2) relative to the cytosolic fraction (lane 1).

More recently, downregulation of tankyrase-1 has been reported to result in severe mitotic defects in prometaphase such as preanaphase arrest, chromosome scattering, and pseudometaphase (Chang et al., 2005a, 2005b). Indeed, tankyrase-1-downregulation (Figure 3B, lane 2) using siRNA (Dynek and Smith, 2004) caused a significant increase of cells in pseudometaphase (Figure 2C), which was reversed by the forced expression of a tankyrase-1 cDNA that contains silent mutations in the target sequence of the siRNA (Figure 3B, lane 3; Figure S4).

These data raised the possibility that p125^{Miki} is Miki that has been PARsylated by tankyrase-1. PAR-antibody immunoblots of anti-PAR immunoprecipitates (of whole-cell extracts) revealed an accumulation of PARsylated polypeptides 9 hr after thymidine release (Figure 3C, top), when cells began to enter M phase as judged by their morphology. In a blot applying the same precipitation products, Miki antibody detected an ~125 kDa band (bottom). Conversely, PAR antibody immunoblots of anti-Miki immunoprecipitates revealed p125^{Miki} in G2/M, but not in G1 cells (Figure 3D, lanes 1 and 2). Downregulation of Miki by siRNA#80 diminished p125^{Miki}, as expected (lane 4). Finally, p125^{Miki} was detected in anti-PAR immunoprecipitates of G2/M-synchronized HeLa cells treated with control siRNA (Figure 3E, lane 1), as expected from the results shown in Figure 3C. However, it was not seen in cells treated with tankyrase-1 siRNA or Miki siRNA#80 (lanes 2 and 3). These data indicate that for a short period during late G2/M phase, p125^{Miki} is in fact PARsylated Miki.

PARsylation of Miki by tankyrase-1 was then tested directly by incubating in vitro-synthesized and purified Miki protein (Figure 3F, lane 2) with tankyrase-1 immunoprecipitated from G1- or G2/M-synchronized HeLa cells (lanes 4 and 5) in the presence of [^{32}P]NAD^{+}. Autoradiographs of the reaction products resolved by SDS-PAGE showed a smear around 120 kDa representing tankyrase-1 PARsylated Miki (lanes 10 and 13). This was no longer seen on treatment with 3-aminobenzamide, a PARP inhibitor (lanes 11 and 14). Intriguingly, tankyrase-1 from G2/M cells PARsylated Miki 4.2-fold more efficiently than that from G1 phase cells (compare lane 10 with 13). This was probably because tankyrase-1 is activated by phosphorylation during the G2/M phase via glycogen synthase kinase (GSK)-3 (Yeh et al., 2006), shown by a migration shift (lane 5, arrowhead).

Both Miki (Figures 1B and 1C) and tankyrase-1 (Chi and Lodish, 2000) localize to the Golgi apparatus (Figure 3G) but did not seem to accumulate in interphasic centrosomes (Figure 1B and Figure 3H). Simultaneous staining of Miki and tankyrase-1 in mitotic cells using the MMC culture method revealed that tankyrase-1-downregulation resulted in diminished Miki fluorescence signals in mitotic centrosomes/spindles (Figure 3I, panel 5, right-hand cell). In contrast, Miki downregulation did not affect tankyrase-1 levels in centrosomes (panel 4, right-hand cell), suggesting that Miki (but not tankyrase-1) in mitotic centrosomes/spindles plays a role in the promotion of prometaphase.

The significance of PARsylation was assessed using the Miki(ΔN) mutant containing silent mutations in the target sequence of siRNA#80. Like the full-length Miki, in vitro-translated

(G) Miki antibody immunoblots of isolated mitotic spindles and centrosomes.
(H) Lysates from HeLa cells (lanes 1, 3, and 5) or lysis buffer alone (lanes 2 and 4) were immunoprecipitated with no antibody (lane 1), control rabbit IgG (lanes 2 and 3), or Miki antibody (lanes 4 and 5). The resulting immunoprecipitates were blotted and reacted with Miki antibody for immunodetection.
(I) A representative result of peptide mass fingerprinting from MALDI-TOF analysis. The molecular weight of each peak and the corresponding amino acid residues of Miki confirmed by MAS sequencing analysis are shown.

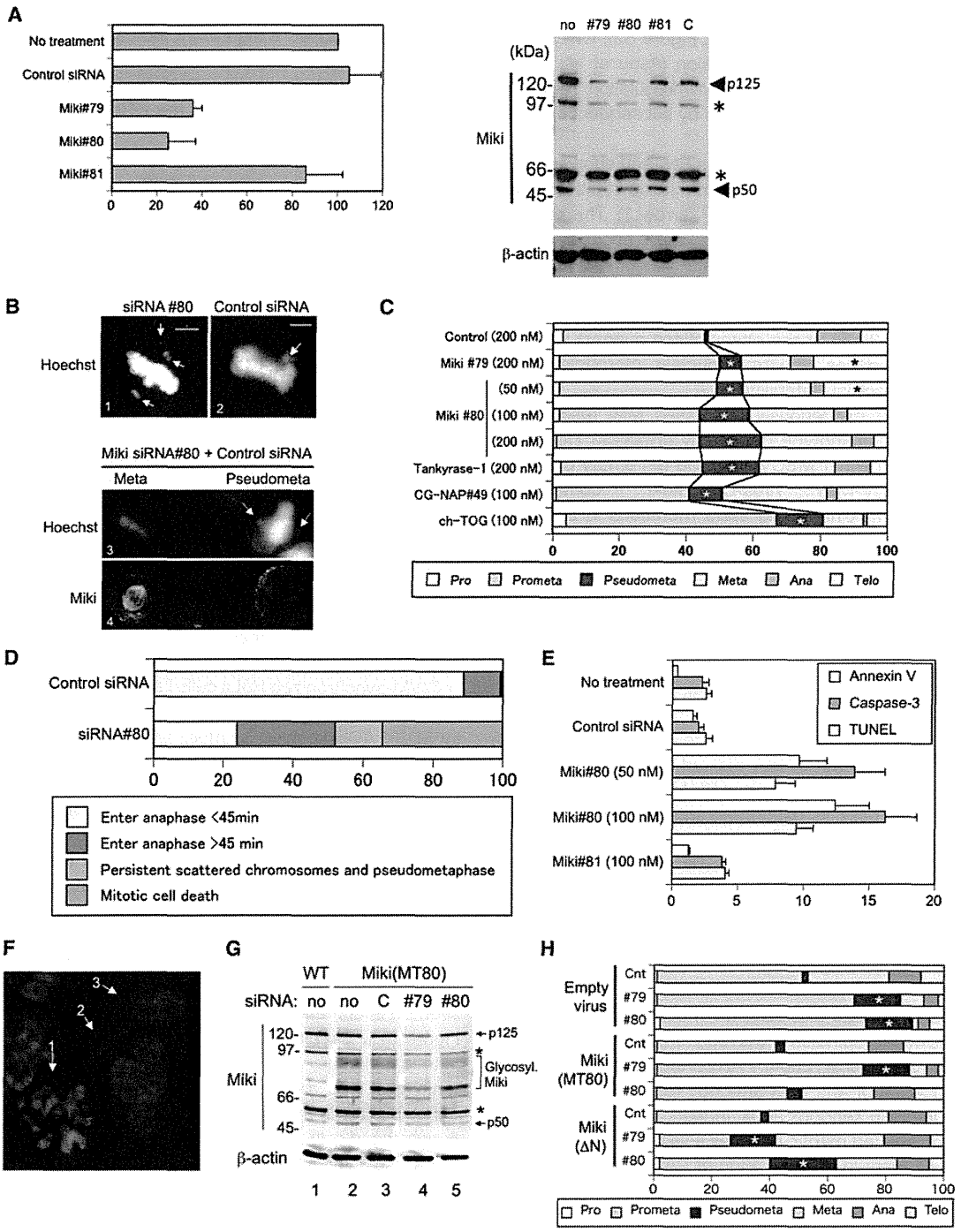

Figure 2. Downregulation of Miki Perturbs Prometaphase

(A) Miki mRNA measured using qRT-PCR and expressed as percent signal relative to an untreated control (left) and Miki or β-actin antibody immunoblots (right) of HeLa cells treated with the indicated siRNA for 24 hr. The mean and SD for four independent experiments are shown (left).

(B) Shown is staining with Hoechst 33342 (panels 1–3) and Miki antibody (panel 4) of mitotic HeLa cells treated with siRNA#80 (panel 1), control siRNA (panel 2), or MMC culture (panels 3 and 4) for 48 hr (100 nM, each).

(C and H) HeLa cells (C) or cells infected either with the MSCV empty retrovirus, virus containing Miki^{MT80}, or Miki(ΔN) cDNA (H) were treated with the siRNA indicated at left for 48 hr (100 nM, except otherwise indicated). Percentages of 200 cells in each mitotic phase or undergoing abnormal mitosis were calculated from observations of Hoechst 33342-stained nuclei. Asterisks indicate a significant increase relative to the control.

Miki(ΔN) protein (Figure 3F, lane 3) can be PARsylated in vitro by tankyrase-1 immunoprecipitated from HeLa cells (lane 17). However, PAR immunoblot analysis of Miki immunoprecipitates revealed that Miki(ΔN) is not PARsylated in vivo (Figure 3J, lane 2). This is different from the full-length Miki, which, as expected, shows a strong $p125^{Miki}$ band (lane 3). Consequently, not only siRNA#79 but also siRNA#80 reduced the levels of $p125^{Miki}$ in cells expressing Miki(ΔN) (Figure 3K, lanes 4 and 5), resulting in a significant increase of the proportion of cells in pseudometaphase by both siRNA#79 and siRNA#80 (Figure 2H).

Downregulation of Miki Reduces the Robustness of Spindles

To investigate the mechanism(s) through which Miki downregulation causes prometaphase disturbance, we monitored the movement of lagging chromosomes in pseudometaphase relative to those in normal late prometaphase. In control siRNA-treated U2OS cells expressing H2B-GFP, all lagging chromosomes in late prometaphase moved toward the metaphase plate at a velocity greater than 1 μm/min, typically 2–5 μm/min (Figure 4A, open bars), consistent with previous reports (Gordon et al., 2001; Levesque and Compton, 2001). In contrast, nearly half of the lagging chromosomes in pseudometaphase cells resulting from siRNA#80 treatment moved less than 1 μm/min (black bars).

Chromosomes may move slowly due to insufficient microtubule tension at kinetochores caused by unfixed (highly motile) spindle poles resulting in synchronous rotation of the chromosomes at prometaphase (Movie S2 and Movie S3) and loss of robustness of mitotic microtubules. α-tubulin staining of siRNA#80-treated cells revealed curling and disorganized spindles, with an occasional chaotic centrosome at only one side of the alignment (Figure 4B). Although spindle microtubules were not visibly fragile, the ratio of tubulin polymers to dimers, a more sensitive measure of spindle strength (Mishima et al., 2004), was reduced to 52% following siRNA#80 treatment for 48 hr compared with cells treated with control siRNA (Figure 4C, compare panel 2 with panel 1). Moreover, low concentrations (1 μM) of nocodazole, a microtubule depolymerizer or short-term cold treatment (5 min) that did not visibly affect mitotic spindles of control cells (compare panels 3 and 5 with panel 1), markedly degraded mitotic spindles of siRNA#80-treated cells (panels 4 and 6).

These findings suggest that Miki downregulation impairs critical a centrosome function(s) such as microtubule nucleation. As demonstrated previously by others (Vaughan, 2005), accumulation of the EB1 microtubule tip-binding protein at centrosomes indicates active microtubule nucleation during mitosis (Figure 4D, panel 1, arrows). The MMC culture method revealed that treatment of HeLa cells with siRNA#80 induced mitotic cells with a pseudometaphase phenotype with markedly reduced centrosomal EB1 signals (panel 2, right-hand cell).

Reduced microtubule nucleation in response to Miki downregulation was also demonstrated in microtubule regrowth assays. Mitotic spindles degraded completely by simultaneous treatment of cells with nocodazole and cold (Figure 4E, panel 1). At this time point, mitotic centrosomes, which are shown as a pair of green dots by γ-tubulin staining (lower right), had several-fold higher intensities than nearby interphasic centrosomes (arrows), as a result of centrosome maturation (discuss in the next section). The cells were then cultured in nocodazole-free medium at 37°C. Within 5 min, 32% of control siRNA-treated mitotic cells showed small asters (<5 μm) forming at centrosomes (panel 2); 8 min later, large asters (>5 μm, panel 3) were observed in 50% of mitotic cells, and numbers increased to nearly 100% within 15 min (panel 4 and bar graph). In contrast, siRNA#80-treated mitotic cells had weaker γ-tubulin signals in centrosomes than cells in interphase (panel 5) and frequently formed multiple small asters (panel 7), and only 16% of mitotic cells showed large asters after 15 min.

The reduced signals of γ-tubulin in mitotic centrosomes and delays of microtubule extension induced by Miki siRNA#80 were rescued by the forced expression of the full-length Miki (panels 9–12), but not by Miki(ΔN) (panels 13–16).

Insufficient Centrosome Maturation Due to Miki Downregulation

The above findings imply that Miki downregulation might impair the γ-tubulin ring complex (γ-TuRC) localizing to the pericentriolar matrix (PCM) that scaffolds microtubule nucleation sites at mitotic centrosomes. Major components of γ-TuRC accumulate in mitotic centrosomes during the short period from late G2 to prometaphase known as "centrosome maturation." For example, the intensity of γ-tubulin immunostaining in prometaphase centrosomes of HeLa cells treated with control siRNA (Figure 5A, arrowheads) increased several-fold relative to those at interphase (arrows). Similarly, other major components of γ-TuRC such as GCP2, kendrin/pericentrin, and CG-NAP/AKAP450 accumulated in mitotic centrosomes (right panel).

To test whether Miki downregulation by siRNA#80 affects signal intensities of these four γ-TuRC components in interphase centrosomes, we transfected Cy3-labeled siRNA#80 into HeLa cells. Prometaphase disturbances including pseudometaphase were induced by Cy3-labeled siRNA#80 and unlabeled siRNA#80 at a similar frequency (data not shown). The intensity of γ-tubulin signals in interphasic centrosomes of Cy3-positive cells (Figure 5B, upper two cells) was essentially the same as in Cy3-negative cells (lower two cells). Indeed, Miki downregulation did not affect signals from four major components of γ-TuRC in interphasic centrosomes (right panel),

(D) U2OS cells that express a histone H2B-GFP fusion protein constitutively were treated with the siRNA (100 nM, indicated at left) for 36 hr. Cells (200 each) that entered prophase were observed for 12 hr.

(E) HeLa cells were treated for 48 hr (for anexinV) or 72 hr (for caspase-3 and TUNEL assay) as indicated at left. Shown is average with SD (four independent experiments) of the percentage of cells positive for annexin-V staining, high caspase-3 activity, or TUNEL assay.

(F) HeLa cells were treated with Miki siRNA#80 for 72 hr. DNA was stained with Hoechst 33342.

(G) Shown are Miki or β-actin antibody immunoblots of HeLa cells (lane 1), cells expressing $Miki^{MT80}$ (lanes 2–5) treated with control siRNA (lane 3), siRNA#79 (lane 4), or siRNA#80 (lane 5). Arrows indicate position of p125, p50; bracket, glycosylated exogenous Miki protein; asterisk, unidentified bands.

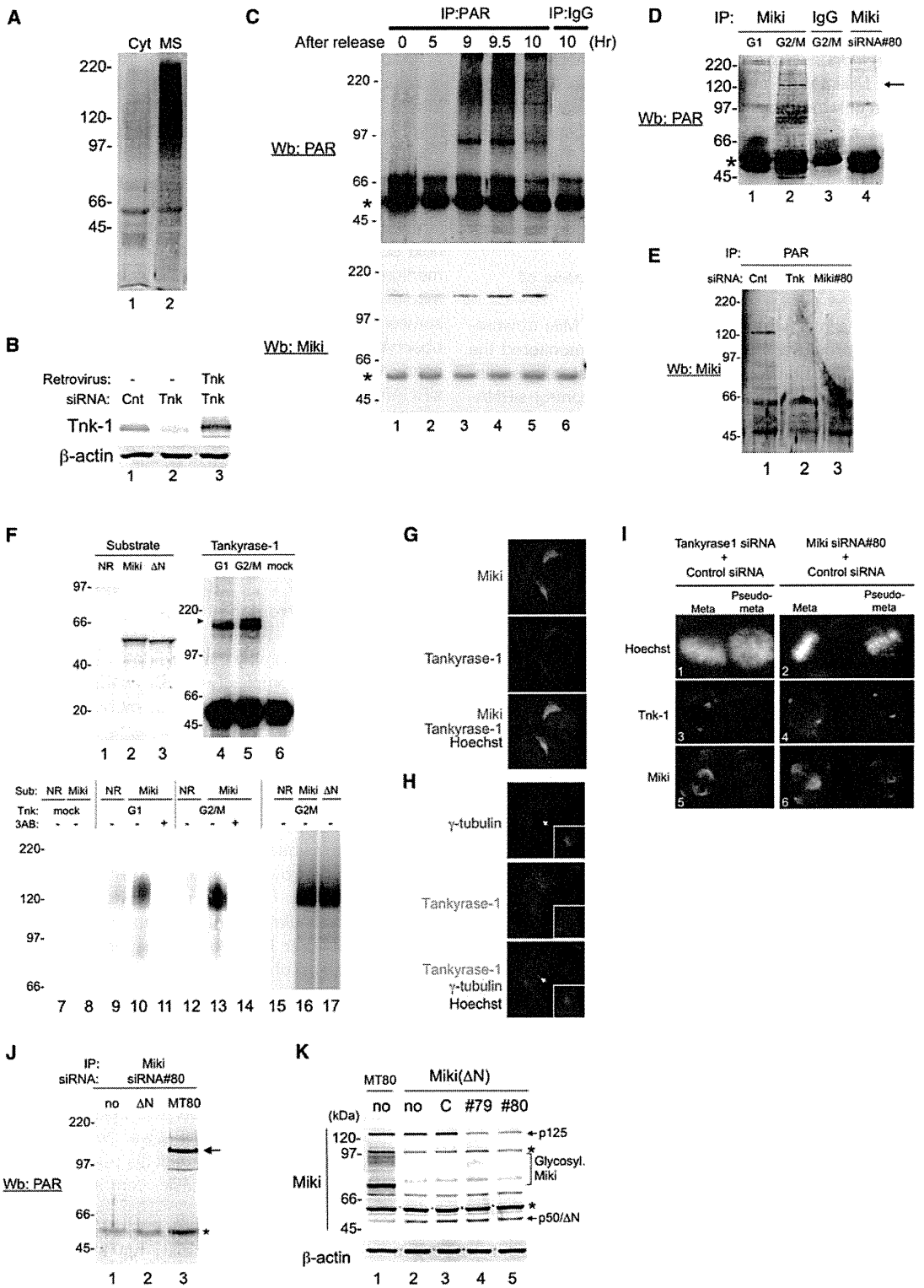

Figure 3. PARsylation of Miki by tankyrase-1

(A) PAR antibody immunoblots of the cytosolic fraction (Cyt) and isolated mitotic spindles and centrosomes (MS) from an equal number of cells.

(B) Immunoblot analysis using tankyrase-1 and β-actin antibodies of whole-cell lysate from HeLa cells (lanes 1 and 2) and cells infected with MSCV-tankyrase-1 (lane 3) treated with control siRNA (lane 1) or siRNA for tankyrase-1 (lanes 2 and 3) (200 nM each for 72 hr).

consistent with the fact that Miki is not present in interphasic centrosomes (Figure 1B).

In contrast to the situation with interphasic centrosomes, Miki downregulation reduced γ-tubulin signals in mitotic centrosomes, as shown by a comparison between those in pseudometaphase (Figure 5C, arrowheads) and those in a nearby interphasic centrosome (arrow). In addition, Miki reduced GCP2 and CG-NAP levels in centrosomes of pseudometaphase even to below those in interphase cells, and prevented the accumulation of kendrin (right panel).

Similarly, downregulation of tankyrase-1, which is necessary for Miki accumulation in mitotic centrosomes (Figure 3I, panel 5), did not affect immunofluorescence signals from γ-TuRC components in interphase centrosomes (Figure 5B, right) but markedly reduced these signals in mitotic centrosomes (Figure 5C, right). Subsequently, tankyrase-1 reduced microtubule nucleation at mitotic centrosomes monitored by EB1 (Figure 4D, panel 3).

To identify the critical γ-TuRC component(s) required for prompt chromosome alignment by PARsylated Miki, we downregulated each component separately by siRNA. CG-NAP downregulation (Figure 5D) caused a significant increase of cells with a pseudometaphase phenotype, in which accumulation of EB1 signals in mitotic centrosomes was not evident (Figure 4D, panel 4). However, the MMC culture method revealed that reduction of CG-NAP did not affect localization of Miki (Figure 5E, panel 5) and tankyrase-1 (panel 6) in mitotic cells. This suggests that CG-NAP is a downstream target of PARsylated Miki to promote progression of prometaphase. In contrast, cells expressing kendrin at reduced levels showed mostly monopolar spindles (data not shown), as previously described by others (Zimmerman et al., 2004), and no significant increase in pseudometaphase (2/200). We could not successfully downregulate γ-tubulin and GCP2.

Finally, we identified ch-TOG/XMAP215, a processive microtubule polymerase (Brouhard et al., 2008) localized to mitotic centrosomes/spindles (Figure 5F, left-hand cells) as a downstream target of PARsylated Miki and CG-NAP. Like major components of γ-TuRC, downregulation of Miki, tankyrase-1, or CG-NAP did not affect fluorescent signal intensity of ch-TOG in interphase centrosomes, but all inhibited accumulation of ch-TOG in mitotic centrosomes (Figure 5G). Conversely, siRNA-mediated downregulation of ch-TOG (Figure 5F, middle panels) did not inhibit centrosomal accumulation of Miki or tankyrase-1 (bottom panels) but caused an increase of prometaphasic cells and pseudometaphase phenotypes to a high frequency (Figure 2C), as predicted by a previous report (Gergely et al., 2003).

Miki Downregulation in Normal Human Primary Cells

To test whether Miki promotes progression of prometaphase in untransformed cells, we downregulated its expression using siRNA#80 in primary cutures of normal human tissues such as retinal pigment epithelial (hRPE) cells (Figure 6A). The number of floating mitotic cells significantly increased from 3.7% (control siRNA-treated cells) to 11.7% (siRNA#80-treated cells) ($p < 0.01$). Hoechst 33342 staining revealed that siRNA#80 induces pseudometaphase (Figure 6B, panel 4) in roughly 6% of mitotic cells (Figure 6C), while no typical pseudometaphase was observed in cells treated with control siRNA. In addition, there was a significant increase of cells at prometaphase and a proportional decrease of those at metaphase, anaphase, and telophase.

Immunostaining revealed that Miki localizes to mitotic spindles in control-siRNA treated hRPE cells (Figure 6B, panel 2). However, in mitotic cells with a pseudometaphase phenotype, Miki signals were barely detectable in mitotic centrosomes and nearby spindles identified by γ-tubulin staining (panel 5). The intensity of γ-tubulin staining in metaphasic centrosomes of control siRNA-treated hRPE cells increased several-fold relative to those at interphase (panel 3), but no enhancement of γ-tubulin signals was seen in cells at pseudometaphase (panel 6), although neither was there a notable decrease (Figure 6D), which is characteristic of siRNA#80-treated HeLa cells (Figure 5C). As a result, spindle formation of hRPE cells at pseudometaphase showed mild disturbances (Figure 6E, panel 6), in contrast to the severe abnormalities frequently seen in siRNA#80-treated HeLa cells (Figure 4B).

Except for the hRPE cells, none of the other normal human primary cells we treated with siRNA#80 showed any mitotic disturbance.

DISCUSSION

We demonstrate that two Golgi proteins, tankyrase-1 and Miki, neither of which is localized to interphasic centrosomes, promote centrosome maturation. In late G2 phase, coincident with the fragmentation of the Golgi apparatus, tankyrase-1 is activated by phosphorylation via GSK-3 (Yeh et al., 2006) and PARsylates Miki, which then translocates to mitotic centrosomes/

(C–E) Cell-cycle phase-enriched HeLa cells (C; D, lanes 1–3) or cells treated with siRNAs indivated above (D, lane 4; E) were subjected to immunoprecipitation (IP) using the antibodies indicated above followed by immunoblot analysis (Wb) using the antibodies indicated. IgG, control mouse IgG. Asterisk indicates position of the immunoglobulin heavy chain.

(F) Tankyrase-1 PARP assay. Coomassie-stained gel with purified in vitro translation products from a no-RNA control (NR, lane 1), Miki mRNA (lane 2), or Miki(ΔN) template. Anti-tankyrase-1 immunoprecipitates from lysates of HeLa cells synchronized at G1 (lane 4) or G2/M (lane 5), and a no-lysate control (mock, lane 6). Autoradiography of PARP-labeled products prepared in the presence or absence of purified substrate (Sub), tankyrase-1 (Tnk), and 3 aminobenzamide (3AB, 1 mM), as indicated above (lanes 7–17).

(G–I) Immunostaining of HeLa cells using antibodies indicated at left. Cells were treated with different siRNAs indicated above (I). DNA was stained with Hoechst 33342. Arrowheads show positions of centrosomes; insets, enlargements of a centrosomal area (H).

(J) HeLa cells (lane 1) or cells expressing Miki(ΔN) (lane 2) or full-length Miki (lane 3) treated with siRNA#80 were subjected to immunoprecipitation (IP) using Miki antibodies followed by immunoblot analysis using PAR antibody. Asterisk indicates position of the immunoglobulin heavy chain.

(K) Miki or β-actin antibody immunoblots of HeLa cells expressing $Miki^{MT80}$ (lane 1), cells expressing Miki(ΔN) (lanes 2–5) treated with control siRNA (lane 3), siRNA#79 (lane 4), or siRNA#80 (lane 5). Arrows indicate position of p125, p50 or Miki(ΔN); bracket, glycosylated exogenous Miki protein; asterisk, unidentified bands.

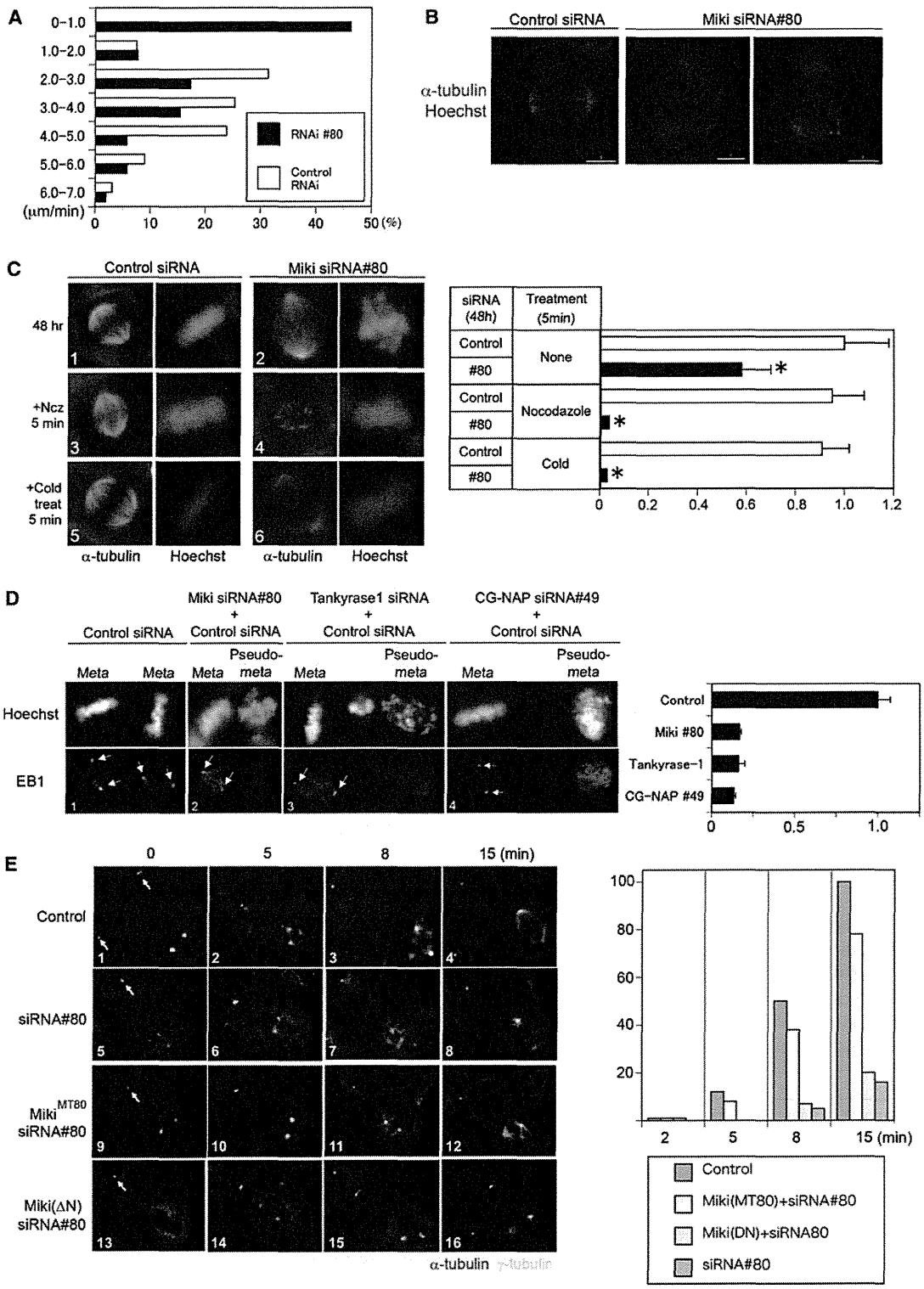

Figure 4. Fragility of Mitotic Spindles in Cells Expressing Low Levels of Miki

(A) Histogram representing the percent (x axis) of H2B-GFP-expressing U2OS cells treated with either 100 nM control siRNA (open bars) or siRNA#80 (black bars) in each 1 μm/min category of lagging chromosome velocity (at left). For calculations of maximum velocity (μm/min), photographs were taken every 15 s over each 15 min observation period.

spindles. Analysis using the Miki(ΔN) mutant revealed that localization of Miki in the Golgi apparatus is necessary for PARsylation and translocation to mitotic centrosomes and spindles.

During the process of centrosome maturation, components of γ-TuRC are rapidly transported and anchored to centrosomes through divergent pathways (for review, see Blagden and Glover, 2003). γ-tubulin, GCP2, and/or GCP3 form a complex called the small γ-TuRC (γ-TuSC) in the cytosol, whereas CG-NAP and kendrin, cognate giant scaffold proteins that share coiled-coil structures, are transported to centrosomes by the dynein/dynactin motor complex. γ-TuSC is then anchored to centrosomes through association of GCP2/GCP3 with CG-NAP/kendrin to form γ-TuRC (Keryer et al., 2003; Takahashi et al., 2002).

Although CG-NAP and kendrin form a complex to provide a platform for γ-TuRC, the roles of each protein are likely to differ because specific suppression of CG-NAP by siRNA disturbs prometaphase through loss of microtubule nucleation, whereas kendrin downregulation causes monopolar spindle formation (Zimmerman et al., 2004). In addition, we recently reported that CG-NAP is connected with the centrioles by interacting with Cep72 (centrosomal protein 72 kDa) (Oshimori et al., 2009). The latter is a previously uncharacterized protein that forms complexes with Kizuna to maintain the integrity of mitotic centrosomes and protect PCM from fragmentation by microtubule-mediated forces (Oshimori et al., 2006). These data suggest that CG-NAP, rather than kendrin, provides a platform for localizing γ-TuRC near centrioles. Downregulation of tankyrase-1 or Miki reduces CG-NAP to barely detectable levels in mitotic centrosomes, while kendrin is maintained at levels similar to those in interphase centrosomes (Figure 5C). This suggests that Miki mainly contributes to CG-NAP-mediated γ-TuRC formation and subsequent microtubule nucleation processes that promote progression of prometaphase.

Severe disturbance of prometaphase was readily induced by Miki downregulation using two siRNAs (siRNA#79 and siRNA#80) or short-hairpin RNA (Asou et al., 2009), each of which targets a different sequence in different human cancer cell lines including HeLa, U2OS, and K562 leukemia cells. We also treated a series of human primary cells with siRNA#80 but found that of these, only hRPE cells showed definite but still relatively mild disturbances at prometaphase (Figure 6). In addition, mice lacking the *Miki* gene do not show apparent abnormalities, and cell lines established from them divide normally (our unpublished data using mice that we generated).

These differences in the effects of Miki downregulation between human and mouse cells or between cancer and untransformed cells suggest that the essential function of Miki anchoring γ-TuRC to mitotic centrosomes can be to a greater or lesser extent substituted by another factor(s). Indeed, members of γ-TuRC including γ-tubulin are readily detected by immunostaining in interphasic centrosomes (Figure 5A) where tankyrase-1 and Miki appear to be absent. Miki downregulation reduces γ-tubulin in mitotic centrosomes to barely detectable levels in HeLa cells (Figure 5C), whereas γ-tubulin in siRNA#80-treated hRPE cells under pseudometaphase conditions is maintained at levels of interphasic centrosomes (Figures 6B, 6D, and 6E), though not enhanced. These findings suggest that HeLa cells may have lost a tankyrase-1/Miki-independent mechanism(s) to anchor γ-TuRC to mitotic centrosomes.

Alternatively, cancer cells may harbor defects of multiple factors in the tankyrase-1/Miki-dependent system for centrosome maturation. For instance, as we previously reported (Asou et al., 2009), low Miki expression levels in MDS cells relate to so-called colchicine-mitosis (scattered and lagging chromosomes) and subsequent abnormal nuclear morphology (binuclei, trinuclei, or multiple nuclei with micronuclei) that characterize MDS. Intriguingly, the CG-NAP gene (1.2 Mb centromeric to *Miki* in band 7q21) also maps to a region frequently deleted in MDS; ~20% of MDS patients lose one allele of both *Miki* and *CG-NAP* genes. This indicates that loss of chromosome arm 7q results in low expression of two crucial factors in the tankyrase-1/Miki-dependent system for centrosome maturation, and that this may profoundly impair progression of prometaphase. Detailed mechanisms through which impairment of the tankyrase-1/Miki-dependent system perturbs cancer cell mitosis are now under investigation in our laboratory, because abnormal mitosis directly causes chromosome instability that could determine the fate of cancer patients.

EXPERIMENTAL PROCEDURES

Cell Culture and Gene Transfer

HeLa, U2OS, 293, and their derivative cells were cultured in Dulbecco's modified Eagle's medium supplemented with 10% fetal bovine serum. hRPE cells were purchased from Takara Bio. (Ohtsu, Japan) and cultured according to the manufacturer's directions. The siRNA oligonucleotides for Miki siRNA#79, siRNA#80, and siRNA#81 (Asou et al., 2009); tankyrase-1 (Dynek and Smith, 2004); ch-TOG (Gergely et al., 2003); NuMA (Chang et al., 2005b) or CG-NAP (siRNA#49, 5′-GCUUCUAUUUAGUCACGAA-3′) were transfected into HeLa(tc) (Oshimori et al., 2006), U2OS, or hRPE cells using Oligofectamine (Invitrogen). Pantropic retrovirus was generated according to procedures described elsewhere (Ozaki et al., 2011) using pMSCV (Clontec) and ires-CD8 (*Kuribara et al.*, 1999).

Mixed Mitotic Cell Culture for Immunostaining

Comparison of immunofluorescence signal intensity between cells treated with different siRNAs was performed as follows. Mitotic cells treated with specific siRNA (for Miki, tankyrase-1 or CG-NAP, which causes mitotic arrest)

(B) Immunostaining of HeLa cells treated with the siRNA indicated above using α-tubulin antibody. DNA was stained with Hoechst 33342.

(C) HeLa cells cultured in the presence of control siRNA or siRNA#80 (100 nM each) for 48 hr (top) were treated with 1 μM nocodazole for 5 min (middle), or put on ice for 5 min (bottom) before immunostaining with α-tubulin antibodies. DNA was stained with Hoechst 33342. The average ratio (20 cells) of tubulin polymers to dimers (with SD) is shown on the right.

(D) Immunostaining of HeLa cells treated with the siRNA indicated above using EB1 antibody. DNA was stained with Hoechst 33342. Relative fluorescence intensity (with SD) (100 centrosomes) is shown at right.

(E) Microtubule regrowth assay. HeLa cells (treated with siRNA and transfected with retrovirus indicated at left) were cultured at low temperature and treated with nocodazole to degrade spindles (0 min), then cultured without nocodazole at 37°C for the periods indicated above (α- and γ-tubulin staining). The ratio of mitotic cells harboring large asters (>5 μm) is shown at right (100 cells).

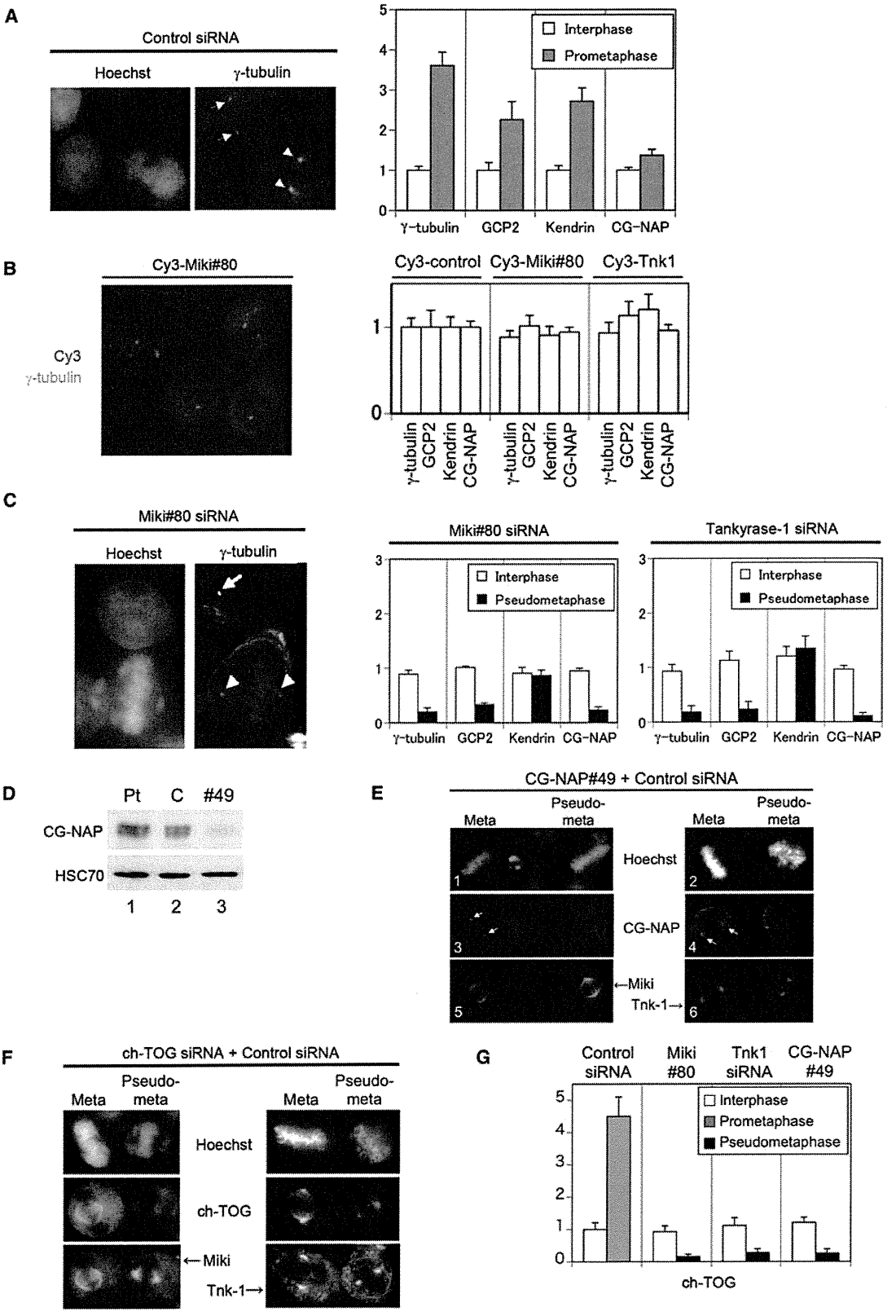
A
Control siRNA
Hoechst
γ-tubulin
Interphase
Prometaphase
γ-tubulin
GCP2
Kendrin
CG-NAP
B
Cy3-Miki#80
Cy3
γ-tubulin
Cy3-control
Cy3-Miki#80
Cy3-Tnk1
C
Miki#80 siRNA
Hoechst
γ-tubulin
Interphase
Pseudometaphase
Tankyrase-1 siRNA
D
Pt
C
#49
CG-NAP
HSC70
1
2
3
E
CG-NAP#49 + Control siRNA
Meta
Pseudo-meta
Hoechst
CG-NAP
←Miki
Tnk-1→
F
ch-TOG siRNA + Control siRNA
ch-TOG
G
Control siRNA
Miki #80
Tnk1 siRNA
CG-NAP #49
ch-TOG